



#### **OPEN ACCESS**

EDITED BY Gianni Ciofani.

Italian Institute of Technology (IIT), Italy

Marisa Freitas,

LAQV Network of Chemistry and Technology, Portugal

Hang Liu,

Chinese Academy of Sciences (CAS), China

Giada Graziana Genchi,

University of Bari Aldo Moro, Italy

\*CORRESPONDENCE

Enrico Mendes Saggioro, ⊠ enrico.saggioro@fiocruz.br

Tommaso Del Rosso,

□ tommaso@puc-rio.br

<sup>†</sup>These authors have contributed equally to this work

RECEIVED 16 March 2025 REVISED 25 July 2025 ACCEPTED 25 September 2025 PUBLISHED 26 November 2025

#### CITATION

Gomes Araujo TB, Concas GC, Gisbert M, Araujo GdF, Boldrini Pereira LdC, Corrêa Maduro LGH, Soares LOS Sales Junior SF, Cunha DP, Correia FV, Laurenzana A, Anceschi C, Frediani E, Chillà A, Margheri F, Del Rosso T and Saggioro EM (2025) Toxicity evaluation of laser-synthesized proangiogenic carbon monoxide-rich gold nanoparticles in vitro and in vivo. Front Bioena Biotechnol 13:1594693 doi: 10.3389/fbioe.2025.1594693

#### COPYRIGHT

© 2025 Gomes Araujo, Concas, Gisbert, Araujo, Boldrini Pereira, Corrêa Maduro, Soares, Sales Junior, Cunha, Correia, Laurenzana, Anceschi, Frediani, Chillà, Margheri, Del Rosso and Saggioro. This is an open-access article distributed under the terms of the Creative Commons Attribution License (CC BY). The use, distribution or reproduction in other forums is permitted, provided the original author(s) and the copyright owner(s) are credited and that the original publication in this journal is cited, in accordance with accepted academic practice. No use, distribution or reproduction is permitted which does not comply with these

# Toxicity evaluation of laser-synthesized pro-angiogenic carbon monoxide-rich gold nanoparticles in vitro and in vivo

Thais Braga Gomes Araujo<sup>1,2†</sup>, Guilherme Conceição Concas<sup>3†</sup>, Mariana Gisbert<sup>3</sup>, Gabriel de Farias Araujo<sup>1</sup>, Leonardo da Cunha Boldrini Pereira<sup>4</sup>, Lorena Gonçalves Henriques Corrêa Maduro<sup>5</sup>, Lorena Oliveira Souza Soares 1.2, Sidney Fernandes Sales Junior 1.2, Davi Pinheiro Cunha<sup>2</sup>, Fábio Veríssimo Correia<sup>1.6</sup>, Anna Laurenzana<sup>7</sup>, Cecilia Anceschi<sup>7</sup>, Elena Frediani<sup>7</sup>, Anastasia Chillà<sup>7</sup>, Francesca Margheri<sup>7</sup>, Tommaso Del Rosso<sup>3</sup>\* and Enrico Mendes Saggioro 1,2\*

<sup>1</sup>Postgraduate Program in Public Health and the Environment, National School of Public Health, Rio de Janeiro, Rio de Janeiro, Brazil, <sup>2</sup>Laboratory for Environmental Health Assessment and Promotion, Oswaldo Cruz Institute. Rio de Janeiro, Rio de Janeiro, Brazil. <sup>3</sup>Laboratory of Laser Synthesis and Characterization of Nanomaterials, Department of Physics, Pontifical Catholic University of Rio de Janeiro, Rio de Janeiro, Rio de Janeiro, Brazil, <sup>4</sup>Division of Metrology in Biology (Dibio), Postgraduate Program in Translational Biomedicine, Postgraduate Program in Biotechnology, National Institute of Metrology, Quality and Technology (Inmetro), Xerém, Directorate of Applied Metrology for Life Sciences - Directorate of Scientific and Technological Metrology (Dimci), Duque de Caxias, Rio de Janeiro, Brazil, <sup>5</sup>Division of Metrology in Biology (Dibio), Postgraduate Program in Biotechnology, National Institute of Metrology, Quality and Technology (Inmetro), Xerém, Directorate of Scientific and Technological Metrology (Dimci), Duque de Caxias, Rio de Janeiro, Brazil, <sup>6</sup>Department of Natural Sciences, Federal University of the State of Rio de Janeiro, Rio de Janeiro, Rio de Janeiro, Brazil, <sup>7</sup>Department of Experimental and Clinical Biomedical Sciences, University of Florence, Florence, Italy

Introduction: The safety profile of gold nanoparticles remains a concern and depends on dose, size, surface chemistry and charge. This study evaluated through in vitro and in vivo methods the cytotoxicity, oxidative stress and genotoxicity of laser synthesized carbon monoxide-Rich Gold Nanoparticles (COR-AuNPs), which can strongly promote angiogenesis in endothelial colony forming cells (ECFC).

Methods: COR-AuNPs were synthesized by pulsed laser driven CO2 reduction reaction, and stabilized for culture media with the addition of the copolymer Pluronic-F127 (PF127). The fresh synthetized nanoparticles where characterized for size and morphology. Their stability was investigated in both culture media and the water aquarium environment. In vitro Cytotoxicity was assessed using the MTS assay on SaOS-2 cells and trypan blue staining in ECFCs at concentrations of 5 and 10  $\times$  10<sup>3</sup>  $\mu g.L^{-1}$ . Zebrafish were exposed to a maximum concentration of 75 µg.L<sup>-1</sup> of COR-AuNPs for 96 h. Oxidative stress biomarkers were assessed in liver and brain tissues, while genotoxicity was evaluated using the comet assay. The analyzed biomarkers included superoxide dismutase, catalase, reduced glutathione, total antioxidant capacity, carbonylated protein, malondialdehyde.

**Results:** The PF127 stabilized COR-AuNPs are stable in the zebrafish aquarium water for 6 weeks and showed no precipitation in the culture media. A strong proangiogenic activity was observed for ECFCs exposed to the COR-AuNPs at a minimal concentration of 5  $\times$  10 $^3$   $\mu g.L^{-1}$ . The CO release is not immediate in the culture medium, suggesting that the COR-AuNPs are characterized by an intracellular release. No significant cytotoxicity was observed in both ECFC or SaOS-2 cells, and most oxidative stress biomarkers showed no significant effects in zebrafish. However, reduced glutathione levels decreased significantly in the brain at concentrations between 10 and 35  $\mu g.L^{-1}$ , likely due to the interaction with the metallic surface of the nanoparticles, while in the liver they increased significantly following exposure to COR-AuNPs at concentrations between 20 and 75  $\mu g.L^{-1}$ . No genotoxic effects were detected in zebrafish.

**Conclusion:** COR-AuNPs enhance capillary morphogenesis in ECFCs, with minimal cytotoxicity, oxidative stress, and genotoxicity at sublethal concentration, supporting their safety for potential applications in regenerative therapies.

KEYWORDS

nanotoxicology, zebrafish, ECFC, angiogenesis, carbon monoxide-rich gold nanoparticles

## 1 Introduction

The fast advancements in bio-nanotechnology have transformed various scientific fields, particularly biomedicine, by enabling the development of innovative materials with unprecedented therapeutic potential (Cabuzu et al., 2015). Among these, about two decades ago new kinds of metal-carbonyl structures denominated carbon monoxide release molecules (CORMs) were proposed to obtain the biological release of carbon monoxide (CO) in cells. The CORMS emerged as a promising treatment material due to their beneficial therapeutic properties (Motterlini and Otterbein, 2010). Although CO is widely known for its high toxicity (Omaye, 2002), due to its affinity for hemoglobin, which is approximately 200 times greater than that of oxygen (Ganong, 1995), it is also produced endogenously by enzymes such as heme oxygenase (Ryter et al., 2006), and plays a crucial role in biological processes, including anti-inflammatory (Tian et al., 2024), anti-apoptotic (Al-Huseini et al., 2014), anti-hypertensive (Penney and Howley, 1991) and antimicrobial activity (Cheng and Hu, 2021). Additionally, it can act as a protective agent in organ transplantation (Clark et al., 2003; Bagul et al., 2008; Nakao et al., 2008; Chen et al., 2009; Yoshida et al., 2010; Romão et al., 2012).

However, the therapeutic application of CO remains challenging, particularly when administered via inhalation (Choi et al., 2022; Yuan et al., 2022). These include a lack of tissue specificity and the need for specialized equipment to monitor *in vivo* CO levels (Queiroga et al., 2015), which can contribute to risks such as hypoxia and high toxicity responses (Omaye, 2002). To mitigate these risks, it is necessary to consider the application of CO within a narrow therapeutic window, typically limited to concentrations of up to 10% of COHb, as previously suggested in the literature (Omaye, 2002; Otterbein, 2009; Chu et al., 2021).

Most CORMs may act as carriers that facilitate the gradual and controlled release of CO. Beyond having a strong anti-inflammatory and antimicrobial effect (Mansour et al., 2022), CORMs have been deeply investigated in regenerative therapies, where the controlled release of CO acts as a signaling molecule that can regulate essential biological processes such as angiogenesis or osteodifferentiation in

human stem cells (Volti et al., 2005; Fayad-Kobeissi et al., 2016; Diomede et al., 2020; Chen et al., 2021; Xu et al., 2023; Nguyen et al., 2024). The CORMs documented in the literature are based on transition metals (Cr, B, Fe, Mn, Co, Mo, Ru, W, Re, Ir) to which CO is covalently attached to form a metal-carbonyl complex (Herrmann, 1990; Motterlini et al., 2002; Nobre et al., 2007; Zhang et al., 2009; Crook et al., 2011; Kautz et al., 2016). This allows CO release through different mechanisms, including pH change, light irradiation, and ligand (Schatzschneider, 2015). Despite the advantages offered by CORMs, their use as pharmaceutical agents presents a number of significant challenges (Otterbein, 2009). A notable disadvantage is that the composition of these compounds, which are based on transition metals such as manganese (Mn) and iridium (Ir), can result in adverse toxic effects within the body (Motterlini et al., 2002; Strigul et al., 2009). A previous study demonstrated that, even in the absence of direct cytotoxicity to cells, the metals used in CORMs can induce DNA damage, thereby posing a considerable risk to patients (Sawicka et al., 2022). Furthermore, many CORMs have to be stored at low temperatures, are chemically unstable in contact with air and have a low solubility in water, which creates several complications for their applicability and storage (Motterlini et al., 2002; 2005; Clark et al., 2003; Romão et al., 2012; Sawicka et al., 2022).

A promising approach to overcome these limitations has been proposed in a recent study, wherein has been demonstrated the feasibility of producing oxocarbon-rich gold nanoparticles by the pulsed laser driven CO<sub>2</sub> reduction reaction (CO<sub>2</sub>RR), where the oxocarbons are constituted by carbon monoxide, formic, acetic, and lactic carboxylic acid (Tahir et al., 2024). A part of the produced nanomaterial is characterized by the presence of carbonyl groups covalently linked to the surface of the gold, being defined as carbon monoxide-rich gold nanoparticles (COR-AuNPs). COR-AuNPs has been recently proved promising for the release of CO *in vitro* e *in vivo* (Chillàet al., 2025), offering a potential alternative to the classical CORMs with highly toxic metal cores (Motterlini et al., 2002; Strigul et al., 2009). In fact, depending on the synthesis conditions, AuNPs are known for their stability in colloidal dispersion, resistance to temperature fluctuations, and low

cytotoxicity, representing an ideal platform for a potential CO release (Balasubramanian et al., 2010; Howe et al., 2013). However, to date, no CORM with a gold metallic part has been synthesized by chemical protocols. Consequently, the COR-AuNPs represent a novel and interesting platform for CO delivery with potential clinical application. In this interesting perspective, as with any nanomaterial intended for a therapeutic use, their comprehensive toxicological assessment is essential to evaluate their biocompatibility and potential risks.

The zebrafish (Danio rerio) has emerged as an invaluable model organism in toxicological and biomedical research (Meyers, 2018). This species offers numerous advantages, including genetic and physiological similarities to humans (Balasubramanian et al., 2010), rapid embryonic development, high reproductive rates, and the transparency of its embryos (Kamstra et al., 2015). Additionally, zebrafish are easy to maintain and handle in laboratory environments, making them highly adaptable for a variety of experimental setups (Arunachalam et al., 2013). These unique characteristics make the zebrafish a versatile and reliable model for studying key toxicological endpoints such as oxidative stress and genotoxicity in vivo (Haque and Ward, 2018). Furthermore, their use has been particularly relevant in assessing the safety and biological effects of nanoparticles (Mutalik et al., 2024), reinforcing their applicability in nanotoxicology and biomedical research (Briggs, 2002; Kamstra et al., 2015).

One of the primary mechanisms underlying nanoparticle toxicity is oxidative stress, which results from an imbalance between the production of reactive oxygen (ROS) and nitrogen (RNS) species and the cellular antioxidant defense system (Mutalik et al., 2024). Excessive reactive species can trigger oxidative damage, leading to lipid peroxidation, protein carbonylation, and DNA strand breaks, all of which contribute to cytotoxic and genotoxic effects (Juan et al., 2021). Given the potential of nanoparticles to induce such responses, genotoxicity evaluations are crucial for understanding the broader implications of nanomaterial exposure (Shukla et al., 2021). Techniques such as the comet assay enable the detection of DNA damage at the cellular level, providing a comprehensive picture of the potential risks posed by nanoparticles (Mahaye et al., 2017). These combined assessments are essential for advancing nanomaterials toward safe biomedical applications. It is important to note that the intrinsic instability of CORMs presents a significant challenge in acquiring cytotoxicity data in complex organisms, creating a lack of information regarding interaction of living systems with these structures (Kautz et al., 2016). In this regard, biological models such as the zebrafish offer a promising approach for the evaluation of novel drugs and the assessment of their suitability for medical applications (Briggs, 2002; Kamstra et al., 2015; Meyers, 2018).

AuNPs, in particular, have been widely studied for biomedical applications due to their tunable physicochemical properties (Mallick et al., 2013) and biocompatibility (Connor et al., 2005). While some studies suggest that AuNPs are less toxic (Browning et al., 2009) and may exert neuroprotective effects (Torres et al., 2021), others have reported embryotoxic effects, including morphological abnormalities and developmental toxicity (Patibandla et al., 2018; Verma et al., 2018). Additionally, some works have highlighted the bioaccumulation of AuNPs in multiple tissues, including the brain, muscle, gills, and digestive tract,

suggesting potential long-term toxicity (Geffroy et al., 2012). In this context, a comparative analysis of the literature, which will be presented in the following sections, can contribute to reveal that factors such as size, surface coating, and concentration play a crucial role in the biological response to AuNPs in studies *in vitro* and *in vivo* with the zebrafish model.

The present study aims to demonstrate different interesting aspects of the COR-AuNPs, such as their stability in complex biological media, their capacity to release CO, their safety profile and their strong pro-angiogenic effect in endothelial colony forming cells (ECFCs) at low minimal concentration, a function critical for tissue vascularization and that might find important applications also in the regeneration of bone tissues (Diomede et al., 2020; Xu et al., 2023). For this reason, we evaluated the degree of cellular toxicity in both ECFCs and bone-derived SaOS-2 cells, as well as oxidative stress and genotoxicity in zebrafish (*D. rerio*) exposed to sub-lethal concentrations. By combining these techniques, this research seeks to provide a critical understanding of the potential risks associated with the use of COR-AuNPs as a novel candidate for regenerative therapies.

### 2 Materials and methods

# 2.1 COR-AuNPs synthesis and characterization

The COR-AuNPs were obtained by pulsed laser driven CO2 reduction reaction with a gold target in water enriched with CO2 by NaOH addition, using an adapted method described elsewhere (Del Rosso et al., 2018; Tahir et al., 2024). In brief, a solution of NaOH at a concentration of 4 mmol.L<sup>-1</sup> was prepared in deionized water. A gold target with a purity greater than 99%, supplied by Kurt J. Lesker, was positioned at the base of a Teflon beaker containing 8 mL of the prepared NaOH solution. PLA was performed for a duration of 6 hours in an open air-liquid interface, employing an Nd:YAG source (Q-Smart 850, Quantel United States) operating at a repetition rate of 10 Hz with a temporal width of 5.8 ns, wavelength of 532 nm, and at a fluence on the target of 3.5 J/ cm<sup>2</sup>. Following the synthesis process, the amphiphilic copolymer Pluronic F-127 (PF127) was added to the colloidal dispersion reaching a final concentration of 2 mg. mL<sup>-1</sup>, to enhance the stability of the colloidal system in an environment with high ionic force or contaminants, such as ammonium compounds present in the system water used for acclimatization, and organic matter derived from fish food and biological debris released by the zebrafish themselves, as demonstrated in (Del Rosso et al., 2018).

The size distribution and morphology of the COR-AuNPs was evaluated by transmission electron microscopy (TEM) JEOL Model 2100F. An inductively coupled plasma mass spectrometer (Nexlon 300X Perkin Elmer, United States) was used to determine the metal concentration in the colloidal dispersion. The presence of the CO-Au bond was identified through the use of a micro-Raman spectrometer (HORIBA XploRA), with the sample previously dried on a glass slide to obtain the surface-enhanced Raman spectra (SERS), similarly as reported in (Muniz-Miranda et al., 2011). This technique is employed as a method to obtain the signal related to chemical bonds at remarkably low

concentrations by exploiting the surface plasmon resonance of the COR-AuNPs, which leads to an enhancement of the electromagnetic field in a confined area near the COR-AuNPs surface. In optimal conditions, this approach can achieve an enhancement in sensitivity to single molecule levels (Kneipp et al., 1997), thus serving as a pivotal method for investigating low-concentration products.

The stability of COR-AuNPs in the zebrafish water environment was evaluated by monitoring the UV-Vis extinction spectra obtained by a double beam Lambda 950 Perkin Elmer spectrophotometer (United States). After the specimens were acclimatized, aquarium water was collected and used as the nanomaterial environment. The colloidal dispersion at concentration of  $42 \times 10^3$  µg.L<sup>-1</sup> was added to the fresh water (50:50 v/v), and the UV-Vis spectra was monitored for 6 weeks at room temperature. The colloidal stability of the COR-AuNPs in cell culture medium was evaluated for 24 h by Dynamic Light Scattering measurement using the intensity distribution as a function of the hydrodynamic diameter. The analysis was carried out at 25 °C using an SZ-100 analyzer from Horiba Instruments (Kyoto, Japan), with a scattering angle of 90°, using a 10 mW laser with a wavelength of 532 nm. For the analysis, the COR-AuNPs were dispersed in a phosphate buffer solution (PBS) with pH 7.4, and RPMI + 10% FBS culture medium at ratio of 3:1 (nanoparticle: culture medium/PBS). COR-AuNPs containing 2 mg.mL<sup>-1</sup> of the amphiphilic block copolymer Pluronic-F127 (PF127) were used for the test.

## 2.2 COR-AuNPs cytotoxicity in SaOS-2 and ECFCs

The SaOS-2 cell line (BCRJ-0217) was obtained from the Rio de Janeiro Cell Bank (https://bcrj.org.br/) packed in frozen ampoules and kept in liquid nitrogen. After thawing, cells were grown in McCoy's 5A medium (Sigma-Aldrich) supplemented with 10% FBS (BioNutrientes) in an incubator at 37 °C in a humidified environment (CellXpert® C170i, Eppendorf, Hamburg, Germany) with 5% CO2 atmosphere. Sterility was ensured by tests for bacteria, fungi, and mycoplasmas. For bacteria and fungi, the cell culture supernatant was placed in thioglycolate (TIO) (Acumedia, Baltimore, United States) and tryptic soy broth (TSB) (Acumedia, Baltimore, United States) and incubated aerobically for 14 days at 22.5 °C ± 2.5 °C and 32.5 °C ± 2.5 °C, respectively. Mycoplasma contamination in the cell supernatants was investigated by bioluminescence using the MycoAlertTM PLUS Mycoplasma Detection Kit (MycoAlert®, Lonza, Verviers, Belgium) and all samples were confirmed to be free of contamination. The cytotoxicity was evaluated according to ISO 19007:2018 - in vitro MTS assay for measuring the cytotoxic effect of nanoparticles. SaOS-2 cells were seeded in 96-well plates at a density of  $3 \times 10^4$  cells per well corresponding to a density of about 93.750 cells per cm<sup>2</sup> (each well ~ 0,32 cm<sup>2</sup>) and maintained for 24 h in McCoy's 5A medium (Sigma-Aldrich) supplemented with 10% FBS (BioNutrientes) in an incubator at 37 °C with a 5% CO<sub>2</sub> atmosphere. Subsequently, the cells were treated with COR-AuNPs at concentrations of 5 and 10  $\times$ 10<sup>3</sup> μg.L<sup>-1</sup>. After 24 h of exposure, the culture medium was discarded, and 200 µL of 0.01 M PBS (Sigma-Aldrich) was added  $(3\times)$  to wash the cells and remove excess nanoparticles. To assess cell viability, the commercial CellTiter 96® AQueous Non-Radioactive Cell Proliferation Assay (MTS) (Promega) was used. The MTS reagent was prepared in phenol red-free culture medium, and 120  $\mu L$  was added to each well across the plate. The incubation time was 1 h at 37  $^{\circ} C$ , after which absorbance was measured at 490 nm using a Biotek Synergy H4 microplate reader (Aligent, Santa Clara, California, United States). After the initial absorbance reading, the supernatant was collected, subjected to centrifugation at 25.155 RCF for 90 min, and absorbance was measured again. This step was designed to minimize potential interferences. There was no significant difference between the readings obtained before and after centrifugation. The negative control consisted of cells cultured in complete medium alone (vehicle). The positive control was performed with 20% DMSO to induce cell death.

Endothelial Colony Forming Cells (ECFCs) were isolated from Human Umbilical Cells (>50 mL) of healthy newborns, as described elsewhere (Margheri et al., 2011; Armanetti et al., 2021), with informed consent from the mothers (R711-D) and observing the Italian legislation (art. 2, paragraph 1, letter f, decree of 18 November 2009). The cells were analyzed by flow-cytometry for expression of the antigens CD45, CD34, CD31, CD105, ULEX, vWF, KDR, and uPAR. ECFCs were cultured in 10% fetal bovine serum (FBS, Euroclone) supplemented EGM2 cell culture media, incubated at 37 °C with 5% CO<sub>2</sub> saturation.

ECFCs were seeded in 6 cm dishes at a density of  $2 \times 10^4$  cells/ cm<sup>2</sup> and cultured in a humidified incubator at 37 °C with 5% CO<sub>2</sub>. After cell attachment, they were incubated with EGM-2 medium (3 mL/well) containing COR-AuNPs at concentrations of  $5 \times 10^3$ and  $10 \times 10^3 \, \mu g \cdot L^{-1}$  for 24 h. Cytotoxicity was determined by trypan blue staining: 20 µL of cell suspensions were resuspended with an equal volume of 0.4% (w/v) trypan blue solution prepared in 0.81% NaCl and 0.06% (w/v) dibasic potassium phosphate. Viable and non-viable cells (trypan blue positive) were counted separately using a dual-chamber hemocytometer and a light microscope. Optical microscopy was used to assess qualitative intracellular uptake of COR-AuNPs. Due to their strong light-scattering properties and high electron density, AuNPs appear as dark, punctate regions within the cytoplasm under brightfield illumination. Cellular images were acquired through the EVOS xl core microscope (AMG, Advanced Microscopy Group).

### 2.3 Intracellular CO release measurement

To assess carbon monoxide (CO) release from the nanoparticles, we quantified carboxyhemoglobin (COHb) levels using a specific ELISA assay. COHb, formed by the binding of CO to hemoglobin, serves as a reliable indicator of intracellular CO presence. For this purpose, we employed human chronic myeloid leukemia K562 cells (DSMZ), which were induced toward erythroid differentiation using 1  $\mu mol.L^{-1}$  Imatinib for 5 days (Jacquel et al., 2003). These cells act as erythroid progenitors capable of synthesizing hemoglobin, providing a biologically relevant model for evaluating CO delivery. Following the treatment, the cells were exposed to 15  $\times$  10³  $\mu g.L^{-1}$  of COR-AuNPs, or to 100  $\mu M$  solution of CORM-2 (Sigma-Aldrich). Cell lysates were analyzed using the COHb ELISA kit (96-well format, MyBioSource, MBS7254040) according to the manufacturer's instructions, enabling sensitive and specific detection of CO-bound hemoglobin within a cellular context that

mimics erythropoiesis. The instructions include a final centrifugation process (at 1000 RCF for 15 min at 2 °C–8 °C), which eliminate the potential interference of the extinction of the AuNPs in the measurement.

# 2.4 COR-AuNPs *in vitro* capillary morphogenesis

In vitro capillary morphogenesis was performed in tissue culture wells with Matrigel (BD Biosciences) coating. A total of 18.000 cells were seeded per well, corresponding to a density of 60.000 cells/cm<sup>2</sup> (well growth area: 0.3 cm<sup>2</sup>) in 2% FBS supplemented EGM-2 culture medium, and incubated at 37 °C at 5% CO2 atmosphere. The pictures were acquired at regular intervals at EVOS optical microscope (Thermo Fisher Scientific, Monza, Italy). The Angiogenesis Analyzer tool of ImageJ software19 provided the statistical analysis for each experimental condition tested quantifying nodes, master junctions and meshes Nodes are identified as pixels that have at least three neighbors, corresponding to a bifurcation. Master junctions are element junctions linking at least three segments. They delimited the master segments". Meshes are the polygon structures reinforced with more than one layer of cells in their walls and have also been referred to by other authors as a "Honeycomb formation".

# 2.5 Set-up for zebrafish acclimatization and COR-AuNPs exposure

This study was approved by the Animal Use Ethics Committee of the Oswaldo Cruz Institute (protocol 035/2022 and license L-001/2023-A1, valid until 2026). Adult zebrafish (*D. rerio*) used in the experiments had an average weight of 0.4 g and length of 3.5 cm. Fish were maintained in glass aquaria with dechlorinated water (pH 7.0–7.6; 23 °C–27 °C), under controlled ammonia levels and a 14:10 h light:dark photoperiod. They were fed with Alcon Neon feed (Alcon, Camboriú, Brazil) via automatic digital feeders. Acclimation lasted 7 days, in accordance with ABNT NBR 15088 guidelines (ABNT NBR, 2022).

Following acclimation, males and females (4.17  $\pm$  0.35 cm; 2.26  $\pm$  0.45 g) were randomly transferred to 36 L exposure aquaria (49.5  $\times$  30  $\times$  24.5 cm), at a density of 1 g of fish per liter. Eighteen fish were placed in each tank, with three replicates per group, totaling 324 animals. Six fish per group were allocated for genotoxicity analysis via the comet assay.

For the acute exposure test, a COR-AuNPs stock dispersion was serially diluted to obtain final concentrations of 5, 10, 20, 35, and 75  $\mu g \cdot L^{-1}$ . All concentrations were sublethal and based on previous toxicological data. Souza et al. (2021) reported complete lethality in zebrafish at concentrations >300  $\mu g \cdot L^{-1}$  of gold nanorods (AuNRs), while 75  $\mu g \cdot L^{-1}$  was considered sublethal. Thus, 75  $\mu g \cdot L^{-1}$  was adopted as the highest test concentration. Additionally, Gong et al. (2016) demonstrated physiological effects without lethality at 60  $\mu g \cdot L^{-1}$  of cobalt in CO-releasing molecules (CORMs), supporting the sublethal design of this experiment. Despite differences in metal core composition, the common mechanism of CO release ensures biological comparability and relevance.

The exposure period lasted 96 h, with solution renewal at 48 h to maintain contaminant levels, establishing a semi-static system (Ge et al., 2015). Control groups were maintained under identical conditions, but without COR-AuNPs.

At the end of the 96-h exposure, fish were euthanized in accordance with ethical guidelines established by the Brazilian National Council for the Control of Animal Experimentation (CONCEA, 2015), and aligned with international standards (Wendy Underwood, 2020; National Cancer Institute, 2023). The procedure was performed by immersion in an ice-water solution (5:1 ratio), maintained between 0 °C and 4 °C. Death was confirmed by the absence of opercular (gill) movements, and the animals were kept in the solution for at least 10 min to ensure complete loss of vital signs. This method was chosen to avoid the use of chemical anesthetics, which could interfere with subsequent biochemical analyses, as previously described by Borski and Hodson (2003).

## 2.6 Tissue collection and homogenization

After euthanasia, liver and brain samples were collected, and 30 mg of each tissue were selected. A total of 1,500  $\mu$ L of 50 mmol·L<sup>-1</sup> potassium phosphate buffer (pH 7.0) was added. The buffer was prepared using ultrapure water, monobasic potassium phosphate (KH<sub>2</sub>PO<sub>4</sub>; Sigma-Aldrich, St. Louis, MO, United States) and dibasic sodium phosphate (Na<sub>2</sub>HPO<sub>4</sub>; Merck, Darmstadt, Germany). The tissue was homogenized for 60 s using a stainless steel spatula. Samples were then centrifuged at 9.400 RCF for 10 min at 4 °C using a 5430R centrifuge (Eppendorf, Hamburg, Germany). The resulting supernatant was transferred to new microtubes (Eppendorf, Hamburg, Germany) and stored at -80 °C until further analysis. The protocol was adapted from Yan et al. (2015) and Yan et al. (2016).

# 2.7 Antioxidant and oxidative stress biomarkers

### 2.7.1 Total protein evaluation

Total protein quantification was performed to standardize the analysis of enzymatic and non-enzymatic biomarkers. The procedure was adapted from Lowry et al. (1951), with modifications by Peterson et al. (2008). After extraction, 20 µL of the resulting sample was mixed with 980 µL of ultrapure water, followed by the addition of 400 µL of reagent A, prepared using sodium hydroxide (NaOH; Sigma-Aldrich, St. Louis, MO, United States), sodium dodecyl sulfate (SDS; Merck, Darmstadt, Germany), and CTC solution containing sodium carbonate (Sigma-Aldrich), sodium potassium tartrate (Isofar, Duque de Caxias, Brazil), and copper sulfate (Dinâmica, Indaiatuba, Brazil), all diluted in ultrapure water. Next, 200 µL of 2N Folin-Ciocalteu reagent (Sigma-Aldrich) was added, and the mixture was incubated in the dark for 30 min. Absorbance was measured at 750 nm using an LTEK INNO microplate reader (Gyeonggi-do, South Korea), and results were calculated based on a BSA calibration curve (bovine serum albumin; Sigma-Aldrich). Data are expressed in  $\mu g \cdot \mu L^{-1}$ .

#### 2.7.2 Superoxide dismutase evaluation (SOD)

The SOD biomarker was quantified using the Superoxide Dismutase Assay Kit (Cayman Chemical Company, Ann Arbor, MI, United States). The reaction mixture consisted of 200  $\mu$ L of radical detector, 50  $\mu$ L of liver or brain extract, and 20  $\mu$ L of xanthine oxidase. The calibration curve was prepared with SOD standards, and absorbance readings were performed at 450 nm using an LTEK INNO microplate reader (Gyeonggi-do, South Korea). Results are expressed as international units of enzymatic activity (U) normalized to protein content (U·g protein<sup>-1</sup>).

#### 2.7.3 Catalase evaluation (CAT)

Catalase (CAT) activity was determined following the protocol by Aebi (1984). Liver samples were diluted 1:10 by mixing 410  $\mu L$  of sample with 3,690  $\mu L$  of ultrapure water; brain samples were not analyzed due to low enzyme activity (Gomes et al., 2019; Araujo et al., 2022). Hydrogen peroxide solution was prepared using hydrogen peroxide (Merck, Darmstadt, Germany) and 50 mmol·L $^{-1}$  potassium phosphate buffer (pH 7.0). Enzyme kinetics were measured by monitoring the decrease in absorbance of  $H_2O_2$  at 240 nm ( $\Delta Abs\ min^{-1}$ ) over 15 s using a UV-Vis spectrophotometer (MS1 model, Bel Photonics, São Paulo, Brazil). Quartz cuvettes were used as blanks and samples. Results are expressed as international units of enzymatic activity (U) per gram of protein.

#### 2.7.4 Reduced glutathione evaluation (GSH)

The GSH concentration was determined using the method established by Wilhelm Filho et al. (2005), with adaptations made for use with a microplate reader. The calibration curve was prepared by adapted for use with a microplate reader. The calibration curve was prepared with concentrations ranging from 0 to 300  $\mu mol \cdot L^{-1}$  from a stock solution of L-Glutathione Reduced (Sigma-Aldrich, St. Louis, MO, United States). A 2x dilution was performed by mixing 400  $\mu L$  of sample with 400  $\mu L$  of ultrapure water. For analysis, 350  $\mu L$  of each calibration standard or sample was mixed with 350  $\mu L$  of 5,5′-dithiobis (2-nitrobenzoic acid) (DTNB; Sigma-Aldrich), incubated in the dark for 15 min, and absorbance was measured at 412 nm using an LTEK INNO microplate reader (Gyeonggi-do, South Korea). Results are expressed in nmol per milligram of protein.

#### 2.7.5 Glutathione-S-Transferase evaluation (GST)

Glutathione S-transferase (GST) activity was determined by measuring the formation of 2,4-dinitrophenyl glutathione (GS-DNB), the product of the conjugation of L-Glutathione Reduced (Sigma-Aldrich, St. Louis, MO, United States) with 1-chloro-2,4-dinitrobenzene (CDNB; Sigma-Aldrich). The method was adapted from Habig et al. (1974). Absorbance was monitored at 340 nm using a UV-Vis spectrophotometer (MS1 model, Bel Photonics, São Paulo, Brazil) over 60 s. Reactions were performed in quintuplicate with different dilutions for liver and brain samples. The reaction mixture was prepared by combining sample aliquots with ultrapure water, phosphate buffer, L-Glutathione Reduced, and CDNB to prevent premature reaction prior to measurement. Enzymatic activity was calculated based on the formation of 1 µmol of GS-DNB per minute and expressed as GST units per gram of protein.

#### 2.7.6 Total antioxidant capacity evaluation (TAC)

Total antioxidant capacity (TAC) was measured using the Trolox equivalent antioxidant capacity (TEAC) method. Phosphate-buffered saline (PBS; 5 mmol·L<sup>-1</sup>, pH 7.4) was prepared using potassium dihydrogen phosphate (KH<sub>2</sub>PO<sub>4</sub>; Sigma-Aldrich, St. Louis, MO, United States) and dipotassium hydrogen phosphate (K<sub>2</sub>HPO<sub>4</sub>; Merck, Darmstadt, Germany). Solutions of ABTS (7 mmol·L<sup>-1</sup>; Merck) and potassium persulfate (2.45 mmol·L<sup>-1</sup>; Sigma-Aldrich) were prepared, and mixed the day before the analysis to form a concentrated solution stored in the dark. On the day of analysis, the mixture was diluted with PBS to an absorbance of 0.700  $\pm$  0.020 at 734 nm and 30 °C, adjusting as necessary. Trolox standard curves (0-0.75 mmol·L<sup>-1</sup>) were constructed. Samples (10 µL of diluted supernatant) were added to the ABTS/potassium persulfate mixture in a microplate, and absorbance was measured at 734 nm and 30 °C using an LTEK INNO microplate reader (Gyeonggi-do, South Korea). Results were calculated by linear regression of the standard curve.

#### 2.7.7 Carbonylated protein evaluation (CPT)

Carbonylated protein (CPT) levels were quantified following the protocol of Mesquita et al. (2014). Briefly, 84 µL of supernatant from each organ (liver and brain) was diluted 1: 5 with ultrapure water. In the microplate, 80  $\mu L$  of 2,4dinitrophenylhydrazine (DNPH;  $10 \text{ mmol} \cdot L^{-1}$ ; Dinâmica, Indaiatuba, Brazil) and 80 µL of sample were added, followed by incubation at room temperature for 10 min. Then, 40 µL of 6 mol·L<sup>-1</sup> sodium hydroxide (NaOH; Sigma-Aldrich, St. Louis, MO, United States) was added, the mixture homogenized by pipetting, incubated for another 10 min, and absorbance read at 450 nm using an LTEK INNO microplate reader (Gyeonggi-do, South Korea). Blanks consisted of 80 µL sample plus 80 µL of 0.5 mol·L<sup>-1</sup> phosphoric acid (H<sub>3</sub>PO<sub>4</sub>; Vetec, Duque de Caxias, Brazil), processed identically. Results are expressed as µmol carbonylated protein per gram of tissue, normalized per gram of protein (μmol·g<sup>-1</sup> tissue per g protein).

#### 2.7.8 Malondialdehyde evaluation (MDA)

Malondialdehyde (MDA) levels were quantified using the TBARS assay kit (Cayman Chemical Company, Ann Arbor, MI, United States) following the manufacturer's protocol. For quantification, 80 µL of supernatant from each organ (liver and brain) was mixed with 80 µL of ultrapure water, followed by the addition of 150 µL of 10% trichloroacetic acid (TCA; Merck, Darmstadt, Germany) and 1,200 µL of 0.53% thiobarbituric acid (TBA; Merck). The TBA solution was prepared by diluting TBA in a 1:1 solution of 20% acetic acid (Merck) and 0.7 mol·L<sup>-1</sup> sodium hydroxide (NaOH; Merck). Calibration curves were constructed using MDA standards (1–70 µmol·L<sup>-1</sup>) prepared in ultrapure water and treated identically. Samples and standards were incubated at 90 °C for 1 h in a thermoblock (Benfer B-BTB, São Paulo, Brazil), followed by an ice bath for 10 min and centrifugation at  $1,600 \times g$  for 10 min at 4 °C using an Eppendorf 5430R centrifuge (Hamburg, Germany). Absorbance was measured at 535 nm using an LTEK INNO microplate reader (Gyeonggi-do, South Korea). Results are expressed as µmol·L<sup>-1</sup> MDA normalized per gram of protein ( $\mu$ mol·L<sup>-1</sup> per g protein).

#### 2.8 Comet assay

Genotoxicity was assessed using the alkaline comet assay, adapted from OECD Test Guideline 489 for the zebrafish (D. rerio) model (OECD Science, 2016). Six fish per experimental group were used, and blood was collected by caudal vein puncture, forming pools by contaminant concentration. Each pool (10 μL) was mixed with 3 μL of heparin (Parinex\*; Hipolabor, Belo Horizonte, Brazil) and embedded in low melting point agarose (LMP agarose; Sigma-Aldrich, St. Louis, MO, United States) at 37 °C. The mixture was applied onto slides previously coated with normal melting point agarose (NMP agarose; Sigma-Aldrich) at 60 °C. After solidification (4 °C  $\pm$ 2 °C), slides were lysed for 24 h at 4 °C ± 2 °C in a buffer containing sodium chloride (2.5 mol·L<sup>-1</sup>; Synth, Diadema, Brazil), EDTA (0.1 mol·L<sup>-1</sup>; Vetec, Duque de Caxias, Brazil), Tris (0.01 mol·L<sup>-1</sup>; Sigma-Aldrich), Triton X-100 (Sigma-Aldrich), and dimethyl sulfoxide (DMSO; Dinâmica, Indaiatuba, Brazil). Electrophoresis was conducted in alkaline buffer (10 mol·L<sup>-1</sup> sodium hydroxide and 0.2 mmol·L<sup>-1</sup> EDTA) at 0 °C-4 °C, with 20 min of DNA unwinding followed by 20 min of electrophoresis at 25 V and 300 mA. Slides were then neutralized with PBS (pH 7.4), fixed in absolute ethanol (Dinâmica), stained with silver nitrate (Sigma-Aldrich), and dried at room temperature. Comet images were captured using an optical (Kasvi-Motic, ×400 magnification) and analyzed using Motic Image Plus 2.0° software. At least 200 nucleoids per slide (five slides per group) were evaluated. DNA damage was assessed based on tail intensity, tail moment, and classified using a five-grade scale (0-4), according to Noroozi et al. (1998). Negative controls consisted of animals maintained in aquarium water under the same experimental conditions, without exposure to COR-AuNPs (see Supplementary Figure S1 in Supplementary Material). Although a positive control was not included in this experiment, our group routinely validates the assay using methyl methanesulfonate (MMS; Sigma-Aldrich) in various models, ensuring methodological reliability. This assay was performed following a protocol previously validated by our group (Sales Junior et al., 2020; 2021; 2024), in accordance with the Minimum Information for Reporting on the Comet Assay (MIRCA) guidelines (Møller et al., 2020), ensuring reproducibility and transparency of the results (Supplementary Table S1 on Supplementary Material).

## 2.9 Statistical analysis

All statistical analyses were performed using GraphPad Prism software (version 9.5.1; GraphPad Software, San Diego, CA, United States). Data normality was assessed using the Shapiro–Wilk test ( $\alpha=0.05$ ). For datasets with normal distribution, one-way ANOVA followed by Dunnett's multiple comparisons test was applied. In cases where normality was not confirmed, non-parametric analyses were conducted using the Kruskal–Wallis test followed by Dunn's *post hoc* test. All biomarker datasets from the zebrafish experiments failed to meet the normality assumption and were therefore analyzed using non-parametric methods. Results are expressed as median  $\pm$  standard error of the mean (SEM), and statistical significance was set at p <

0.05. For the SaOS-2 assays, data normality was verified using the Shapiro-Wilk test, followed by one-way ANOVA with multiple comparisons. Results are presented as mean percentage values relative to non-exposed control wells (considered as 100%), which were cultured in medium alone.

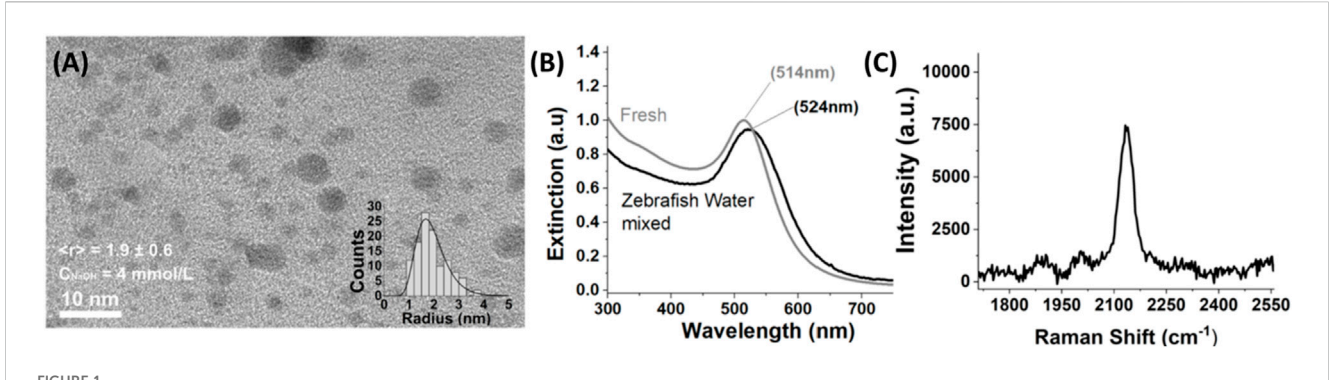
## 3 Results and discussion

## 3.1 COR-AuNPs characterization and CO release

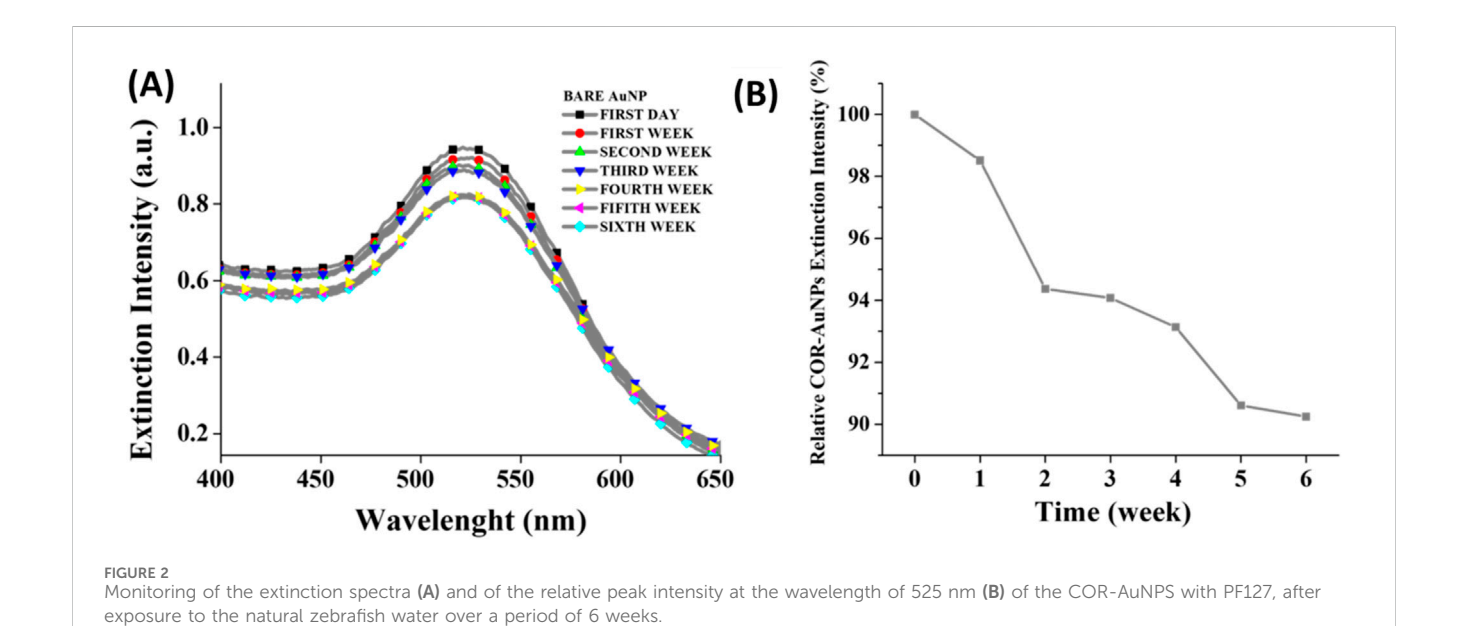
The PLA process resulted in the formation of well-defined spherical nanoparticles with a narrow distribution, measuring less than 10 nm (Figure 1A). As the synthesis process was performed in batch without a water flowing system, the nanoparticles were also subjected to laser fragmentation in liquid subsequent to their production, resulting in the formation of ultrasmall nanoparticles with an average radius of 1.9 nm, as previously reported (Tahir et al., 2024).

As stated in the introduction, the pulsed laser driven CO<sub>2</sub> reduction reaction results to the synthesis of gold nanoparticles rich in CO (Del Rosso et al., 2016) and organometallic nanocomposites constituted by gold nanoclusters embedded in formic, acetic and lactic acids, with concentrations of about 0.3, 1.4, and 0.2 ppm, respectively (Tahir et al., 2024). The UV-Vis spectra of the pristine colloidal dispersion of nanoparticles exhibit the characteristic localized surface plasmon resonance (LSPR) peak at 514 nm, which shifts to 524 nm after the addition of the amphiphilic copolymer block Pluronic-F127 (PF127) and the subsequent incubation in the zebrafish aquarium. As visible in Figure 1B, the shape and full width half maximum (FWHM) of the LSPR curve is not affected by the zebrafish water environment, and we only notice a slight decrease in the intensity of the maximum, probably associated to a small portion of nanoparticles (less than 10%) precipitated after the incubation in the aquarium. The SERS measurement demonstrated the existence of gold-carbonyl (Au-CO) chemical bonds, thereby confirming the presence of CO associated with the COR-AuNPs (Figure 1C).

The copolymer PF127 was utilized as a method to enhance the stability of the COR-AuNPs, as demonstrated in previous study (Del Rosso et al., 2018). In addition to the afforementioned effect, PF127 has applications as a drug delivery system (Moore et al., 2000), facilitating the penetration of nanocomposites into cancer cells (Elagin et al., 2014; Simon et al., 2015). In this study, we assess the stability of the NPs in zebrafish aquarium water by monitoring the variation in intensity of the extinction peak of the COR-AuNPs (Figure 2A) over a 6-weeks period. It can be observed that the NPs were markedly stable, with the peak extinction reducing by only 6% over the course of the experiment (1 week), and by only 10% within 6-weeks (Figure 2B), while the FWHM had a variation of 0.8% and 7.6% indicating minimal agglomeration after their dispersion in the zebrafish water (Sangwan and Seth, 2022). The physicochemical stability of the COR-AuNPs is a fundamental requirement for their applicability in biological systems (Sharma et al., 2021), as instability can lead to aggregation, which in turn alters the nanoparticle's biodistribution, bioavailability, and potential toxicity (Abbasi et al., 2023).



(A) TEM images of the colloidal dispersions of COR-AuNPs synthesized by PLA at air-water interface with a concentration of NaOH ( $C_{NaOH}$ ) of 4 mmol.L<sup>-1</sup>. In the inset is represented the statistical size distribution. (B) UV-Vis spectra of the colloidal dispersions of COR-AuNPs before (fresh-grey line) and after the addition of PF127 followed by the incubation in the zebrafish aquarium. (C) SERS spectra obtained from the analysis of a few drops of COR-AuNPs dried on silicon substrate. The Au-CO peak (2,124 cm<sup>-1</sup>) is highlighted.

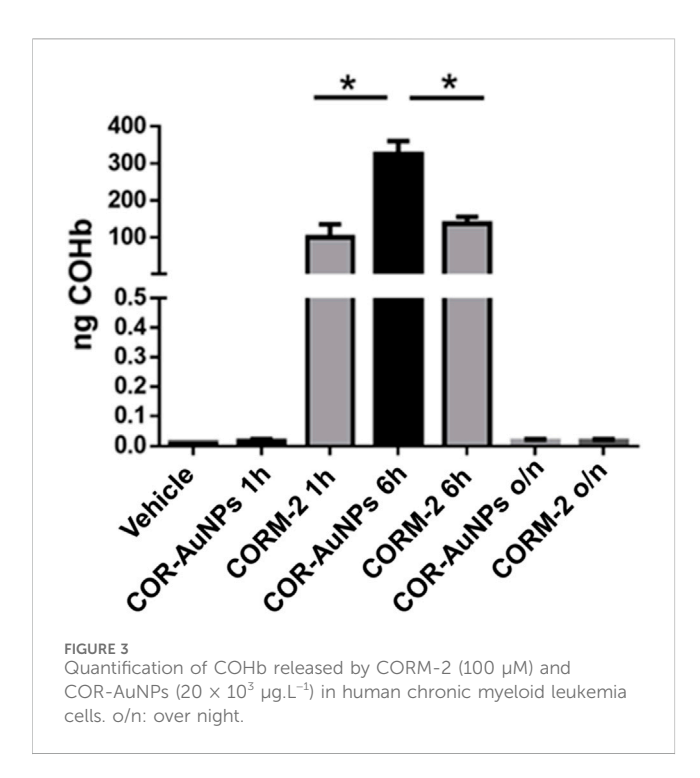


A dynamic light scattering (DLS) analysis of COR-AuNPs in phosphate buffered saline (PBS) and McCoy's 5A cell culture medium supplemented with fetal bovine serum (FBS) measurements were taken at 0 h for both conditions, and after 24 h for COR-AuNPs in McCoy's 5A + FBS. Peaks centered at 13 nm and 49 nm were observed for COR-AuNPs in PBS and cell culture medium, respectively, indicating a possible interaction with FBS. Following a 24-hour period of incubation in cell medium, we observed a small shift of the peak to 51 nm, indicating that the COR-AuNPs functionalized by PF127 are stable in complex biological media (Supplementary Figure S2 on Supplementary Material).

The characterization of the COR-AuNPs was completed by measuring the release of CO in cells using the Elisa COHb test on human chronic myeloid leukemia cells (K562). The results of CO release are reported in Figure 3, showing the formation of COHb when K562 cells were treated with both CORM-2 and COR-AuNPs. The CO release profiles exhibited significant variation over the

duration of one hour. The release rate of CORM-2 was found to be accelerated, and after a duration of 6 h, the concentration of COHb was observed to be elevated in the presence of COR-AuNPs. The ensuing results illustrate the disparities in the time-dependent mechanisms of CO release for the structures in question. Indeed, extant literature on the subject indicates that the release of carbon monoxide (CO) by CORM-2 occurs extracellularly and commences within minutes of its dispersion in the culture medium (Southam et al., 2021). Conversely, the COR-AuNPs necessitated a duration exceeding 60 min for the identification of COHb, thereby indicating an intracellular initiation of the CO release process.

The laser-synthesized COR-AuNPs presented herein offer several advantages over most commercial CORMs that frequently contain toxic metals (e.g., Cr, B, Fe, Mn, Co, Mo, Ru, W, Re, Ir) (Herrmann, 1990; Motterlini et al., 2002; Nobre et al., 2007; Zhang et al., 2009; Crook et al., 2011; Kautz et al., 2016), require protection from light, must be stored at –20 °C (Pizarro et al., 2009; Crook et al., 2011), and present low solubility in water (Motterlini et al., 2002;



Bannenberg and Vieira, 2009). In contrast, the synthesis of COR-AuNPs employs a one-step, eco-friendly technique that utilizes solely gold, water and aqueous CO<sub>2</sub>. These nanoparticles exhibit stability at room atmosphere and can be stored at room temperature on the shelf, as evidenced by the COHb levels measured after a few months of storage, that remained consistent, indicating the preservation of the CO release property (Chillàet al., 2025).

# 3.2 Cytotoxicity and pro-angiogenic activity of the COR-AuNPs *in vitro*

Considering the prospective applications of CO delivery systems in the treatment of vascular diseases (Dulak et al., 2008; Choi et al., 2022), we assessed the cytotoxicity of the nanoparticles in endothelial colony forming cells (ECFCs), a subtype of Endothelial Progenitor cells (Figures 4A,B), as well as in the osteogenic sarcoma cell line SaOS-2.

To further investigate their impact on angiogenesis, a capillary morphogenesis assay was performed using ECFCs. This assay evaluated both nanoparticle uptake (Figure 4C) and their effect on the formation of capillary-like structures (Figure 4D). A clear increase in the number of master junctions, meshes, and master nodes (Figure 4E) was observed. As illustrated in Figures 4A,B, the cells were exposed to vehicle or COR-AuNPs at concentrations of 5 and  $10 \times 10^3$  µg.L<sup>-1</sup>, and no toxicity was observed after 24 h of incubation. The outcomes can be attributed to the laser synthesis process (Tahir et al., 2024), which does not involve the use of toxic solvent or reagents, and relies exclusively on the physical interaction between light, the target, and the molecules in the liquid environment. These results are consistent with our previous studies on RAW267.4, NCTC and HMVEC cells (Tahir et al., 2024).

In addition to ECFCs, we investigated the effects of COR-AuNPs on SaOS-2 osteosarcoma cells, that did not show cytotoxic potential

since the cell solutions offered relative viability greater than 70% in all conditions tested after 24 h of exposure (Figure 4B), when compared to the negative control (untreated cells). Considering that effective bone regeneration is closely linked to neovascularization (Dalle Carbonare et al., 2025), this approach aims to explore the potential applicability of these nanoparticles in regenerative therapies across different tissue types.

## 3.3 Toxicology investigation in vivo

#### 3.3.1 Antioxidant biomarkers

The zebrafish model provides additional insights into the *in vivo* effects of COR-AuNPs, particularly concerning oxidative stress, a key parameter in nanotoxicology (Horie and Tabei, 2021). Oxidative stress occurs when the balance between the production of reactive oxygen and nitrogen species (ROS/RNS) and antioxidant defense mechanisms is disrupted (Lushchak and Storey, 2021), which may result in biomolecular harms (Roberts et al., 2010). In this study, we evaluated multiple oxidative stress biomarkers to assess potential disturbances in cellular homeostasis induced by COR-AuNPs exposure.

The activity of the enzyme SOD was evaluated in the brain and liver of fish exposed to different concentrations of COR-AuNPs (Figure 5A). No significant changes in SOD activity were observed in the brain at any concentration. In the liver, a substantial decrease in SOD activity was observed at a concentration of 5  $\mu g \cdot L^{-1}$ , while no statistically significant differences were detected at other concentration when compared to the control.. This pattern may suggest reduced bioavailability at higher concentrations, leading to diminished biological effects (Lim et al., 2024). Alternatively, the reduction at 5  $\mu g \cdot L^{-1}$  could represent a random variation without indication of toxicity.

As ilustrated in Figure 5B below, the activity of the enzyme catalase (CAT) in fish exposed to COR-AuNPs is demonstrated. As reported in the literature, CAT activity is typically reduced in the brains of these animals (Gomes et al., 2019; Araujo et al., 2022), which led us to focus the analysis exclusively on the liver. The stability of these enzymes across most tested COR-AuNPs concentrations suggests that, despite the reduction in SOD activity at lower concentrations, the antioxidant system maintained redox equilibrium (Krishnamurthy et al., 2024). Give SOD catalyzes the dismutation of the highly reactive superoxide radical (O<sub>2</sub>-·) into hydrogen peroxide (Zheng et al., 2023), which is subsequently decomposed into water and molecular oxygen by enzymes such as CAT (Anwar et al., 2024), the observed stability in these biomarkers indicates that COR-AuNPs do not significantly disrupt these antioxidant defenses under the tested conditions (Vona et al., 2019). In a previous work, gold nanoparticles synthesized by the seeded growth method (Murphy and Jana, 2002) were assessed for their effects on various biological parameters, including the gene expression of SOD and CAT. The results showed a significant increase in the expression of these enzymes following exposure to the nanoparticles. SOD expression was elevated after exposure to 0.01 nM AuNRs (gold nanorods) (1.97 μg.L<sup>-1</sup>), while CAT expression increased with both 0.01 nM GNRs (1.97 µg.L<sup>-1</sup>) and 0.05 nM PAH-PSS-AuNRs (gold nanorods coated with polyallylamine hydrochloride, PAH) (9.85 µg.L<sup>-1</sup>)

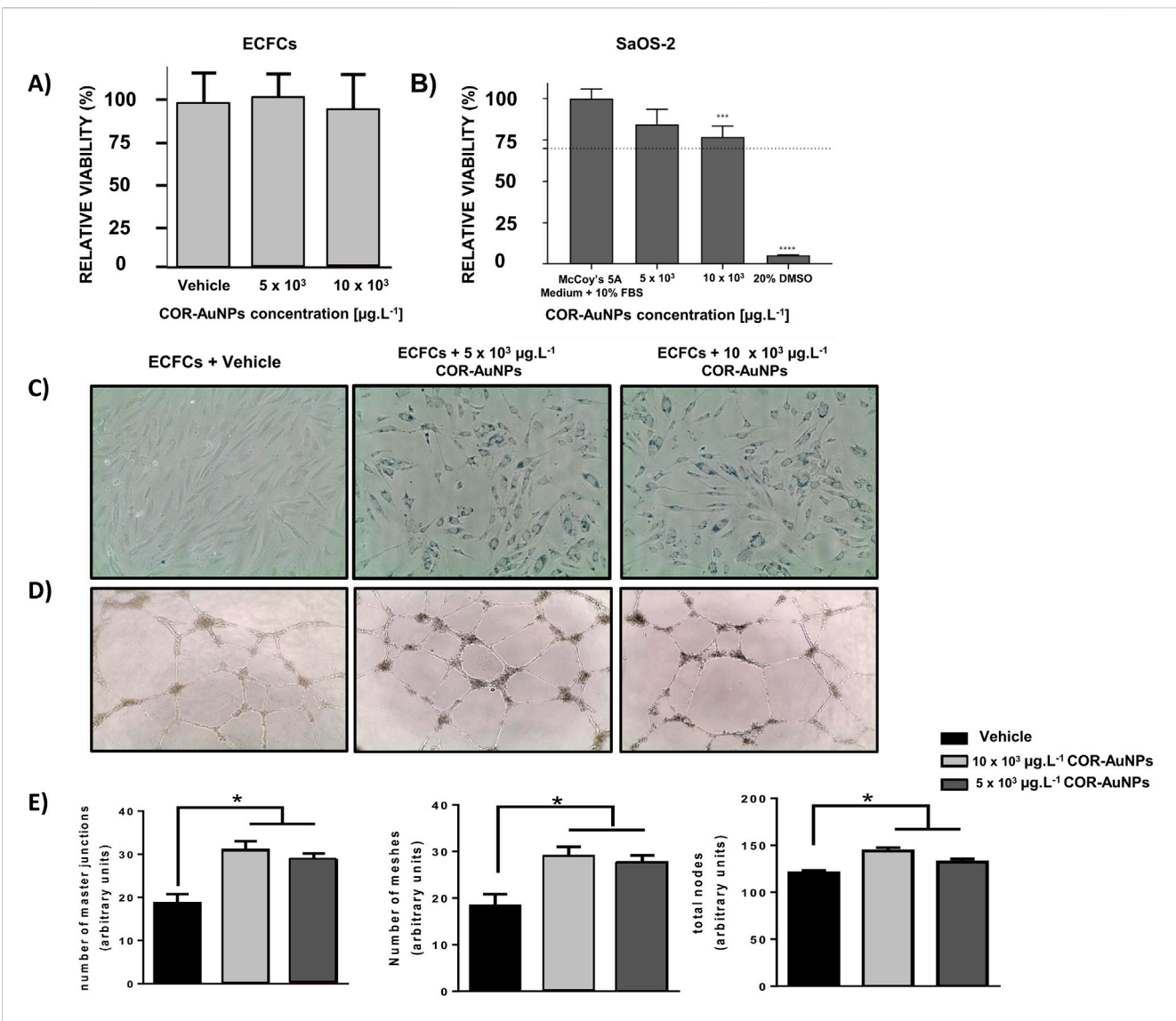


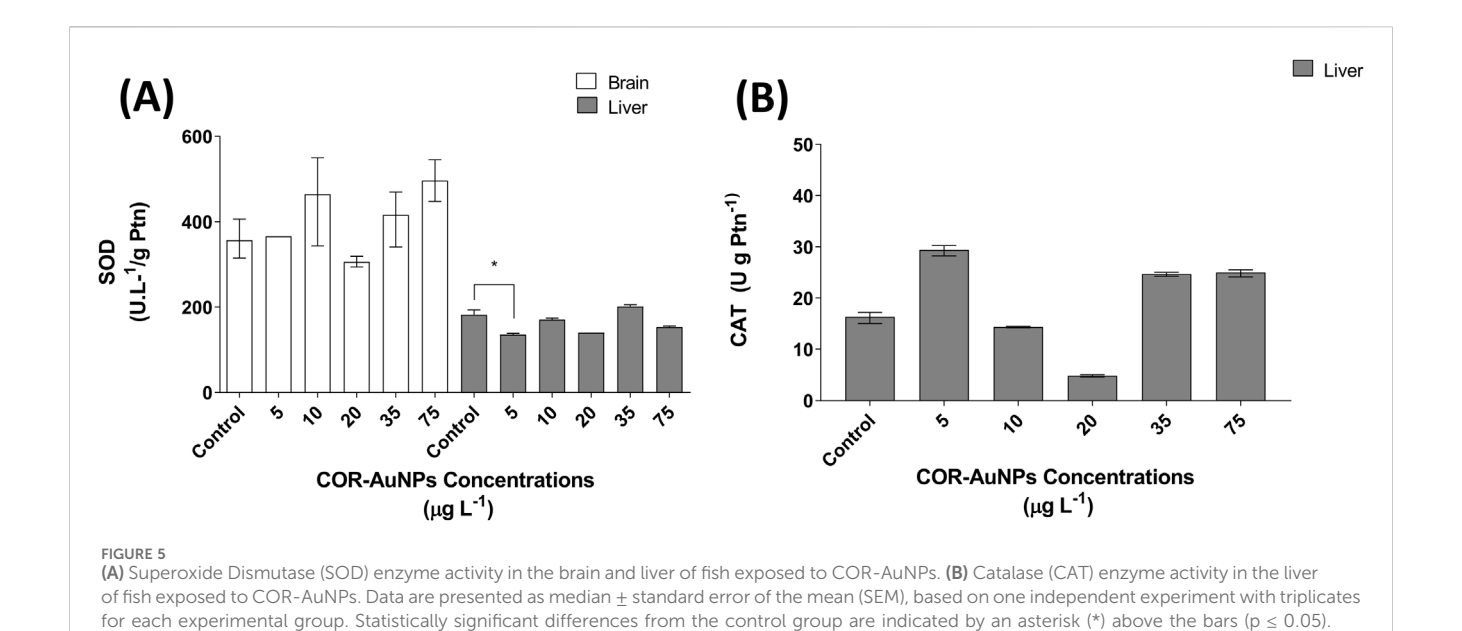
FIGURE 4
(A) Relative viability of ECFCs treated with COR-AuNPs for 24 h, performed by trypan blue assay. For statistical analysis the data were analyzed using GraphPad Prism6 and Origin and expressed as a mean value  $\pm$  SD. Statistical analysis was performed using One way Anova. (B) Relative viability of SaOS-2 cells exposed (24 h) to the COR-AuNPs (5 and  $10 \times 10^3 \ \mu g.L^{-1}$ ) in McCoy's 5A medium + 10% FBS (vehicle; positive control of cell death (DMSO 20%). The dashed line represents 70% relative viability. Values below this line are considered indicative of cytotoxic effects. Statistically significant differences compared to the controls for each time point are indicated by an asterisks above the bars (\*\*\*p < 0.0006 and\*\*\*\*p < 0.0001). (C) Images acquired with optical microscope for ECFCs loaded with COR-AuNPs at different concentrations. The internalized metal loads are identifiable as the dark areas inside the cells (24 h). (D) Optical microscopy images of capillary network structures of ECFCs exposed to two different concentrations of COR-AuNPs (upper panel). (E) The degree of morphogenesis was quantified using the ImageJ software, by evaluation of the number of master junction, nodes and total networks (meshes) branching out from a branch point/node, as reported in the histograms.

(Patibandla et al., 2018). These findings emphasize the influence of nanoparticle shape and coating on toxicity and suggest the low toxicity of the COR-AuNPs synthesized in the present study.

The levels of reduced glutathione (GSH) were assessed in fish exposed to varying concentrations of COR-AuNPs, exhibiting distinct, tissue-specific patterns. In the brain, GSH levels significantly decreased at concentrations of 10, 20, and 35  $\mu$ g.L<sup>-1</sup>, while in the liver, a significant increase in GSH levels was observed at concentrations of 20, 35, and 75  $\mu$ g.L<sup>-1</sup> (Figure 6A). As the most relevant low molecular weight antioxidant produced within cells

(Forman et al., 2009), GSH plays a crucial role in xenobiotic metabolism and in maintaining redox homeostasis, serving as a cofactor for enzymes such as glutathione S-transferase (GST) and glutathione peroxidase (GPX) (Koramutla et al., 2021). The observed modulation of GSH levels suggests that the CORAUNPs can influence the GSH intracellular levels.

Based on the available scientific evidence, it is plausible that the observed reduction in glutathione levels is related to the direct interaction between gold nanoparticles (AuNPs) and intracellular GSH. The affinity of the thiol (-SH) group in GSH for metals such as



☐ Brain (B) Brain (A) Liver Liver 100 80 mmol gPtn<sup>-1</sup>) GST (U.L<sup>-1</sup>/g Ptn) 60 40 20 Control Control 0 Control Control 6 P 20 20 **COR-AuNPs Concentrations** COR-AuNPs Concentrations (μg L<sup>-1</sup>) (μg L-1) (A) Reduced Glutathione (GSH) levels in the brain and liver of fish exposed to COR-AuNPs. (B) Glutathione S-Transferase (GST) enzyme activity in the brain and liver of fish exposed to COR-AuNPs. Data are presented as median  $\pm$  standard error of the mean (SEM), based on one independent experiment with triplicates for each experimental group. Statistically significant differences from the control group are indicated by an asterisk (\*) above the bars (p < 0.05)

gold is well documented, leading to the formation of stable Au–S bonds (Xue et al., 2014; Luo et al., 2016). This interaction may result in GSH depletion, particularly at higher AuNP concentrations, where the organism's GSH synthesis capacity may become overwhelmed. Additionally, research indicates that small-sized AuNPs can enter cells and preferentially bind to GSH thiol groups, leading to a significant decrease in intracellular GSH levels (Sokolsky-Papkov and Kabanov, 2019; Jawaid et al., 2020). In the context of the present study, the synthesis of COR-AuNPs without thiolated ligands, such as citrate or dihydrolipoic acid (DHLA), and the use of Pluronic F-127 as a stabilizing agent, which does not form covalent bonds with gold, may leave part of the AuNP surface exposed. This exposure facilitates interactions with biomolecules *in vivo*, such as GSH, enhancing the formation of

Au–S bonds and contributing to the observed GSH depletion (Xue et al., 2014; Jawaid et al., 2020). Therefore, the hypothesis that GSH is being sequestered by AuNPs, surpassing the organism's synthesis capacity and leading to reduced GSH levels, is consistent with findings in the literature and may explain the results observed in this study. While the direct interaction of AuNPs with GSH thiol groups appears to be a plausible mechanism for GSH depletion, it is not possible to fully exclude the possibility that the decrease reflects a physiological adjustment due to altered redox demand.

Nevertheless, when considering GSH levels in isolation, it is not possible to determine whether the reduction in this biomarker was triggered by a lack of demand or by a suppression resulting from excessive demand that exceeded the organism's capacity for GSH synthesis. It has been demonstrated in prior studies that gold

nanoparticles produced by the modified Turkevich method (6.3 nm) and capped with dihydrolipoic acid (7.3 nm) posses the capability to modulate GSH levels without inducing ROS generation at concentrations ranging from 1 to 6  $\mu g \cdot L^{-1}$ . While these concentrations differ from those utilized in the present study, they demonstrate that GSH modulation may occur independently of ROS overproduction (Tournebize et al., 2012). Similarly, biologically synthesized AuNPs applied at higher concentrations (9.7–58.2 mg · L^{-1}) have been shown to reduce ROS production in zebrafish (Ramachandran et al., 2018). Collectively, these findings lend support to the hypothesis that COR-AuNPs modulate GSH activity as part of an adaptive physiological response, rather than inducing toxicity, even within the concentration range that was evaluated in this study.

On the other hand, increased levels of GSH were observed in the liver at concentrations above 20 µg·L<sup>-1</sup>. This finding may be indicative of an adaptive response aimed at maintaining redox homeostasis. This notion is supported by the established role of GSH in neutralizing reactive oxygen species (ROS) and in the regeneration of other antioxidants through the glutathione redox cycle (Wu et al., 2004). Although the activities of SOD and CAT did not increase to a statistically significant degree, both enzymes demonstrated higher values in comparison to the control group. This trend, though not statistically significant, may suggest a subtle accumulation of reactive oxygen species (ROS) in the liver, which could have triggered a compensatory elevation in GSH synthesis. It is also important to note that increased GSH levels can be beneficial depending on the physiological context, as GSH participates not only in antioxidant defense but also in detoxification processes (Lushchak, 2012) and cellular signaling pathways (Chai and Mieyal, 2023).

Furthermore, the response of Glutathione S-Transferase (GST) activity to these concentrations was investigated. The results demonstrated no statistically significant alterations in GST activity in either the brain or liver, irrespective of the concentration that was examined (Figure 6B). GST plays a pivotal role in the conjugation of glutathione (GSH) with electrophilic species, functioning as a crucial enzyme in the phase II metabolism of xenobiotics (Landi, 2000). However, the results indicated no statistically significant alterations in GST. Conversely, an in vitro study revealed that AuNPs did not induce alterations in GST activity within hemolymph and gill cells of Mytilus galloprovincialis. It is worth noting that, in the context of coexposure with pharmaceuticals such as carbamazepine and fluoxetine, AuNPs demonstrated a protective effect, effectively preventing the enzyme induction triggered by these drugs (Barreto et al., 2019). Unlike previous studies reporting GST activity alterations in fish following the exposure of citrate-AuNPs (35 nm) obtained by Turkevich method and functionalized polyvinylpyrrolidon-AuNPs (50 nm) at a concentration of 80 μg.L<sup>-1</sup> (Luis et al., 2016), our data suggest that the COR-AuNPs synthesized in this study exhibit low biological impact.

Likewise, Total Antioxidant Capacity (TAC), which reflects the synergistic potential of the antioxidant system (Pellegrini et al., 2006) was analyzed in the brain and liver of fish exposed to different concentrations of COR-AuNPs. In the brain, TAC showed no significant variations at any of the evaluated concentrations. In the liver, a significant decrease in TAC was observed at the concentration of 75  $\mu g.L^{-1}$ , while the other concentrations

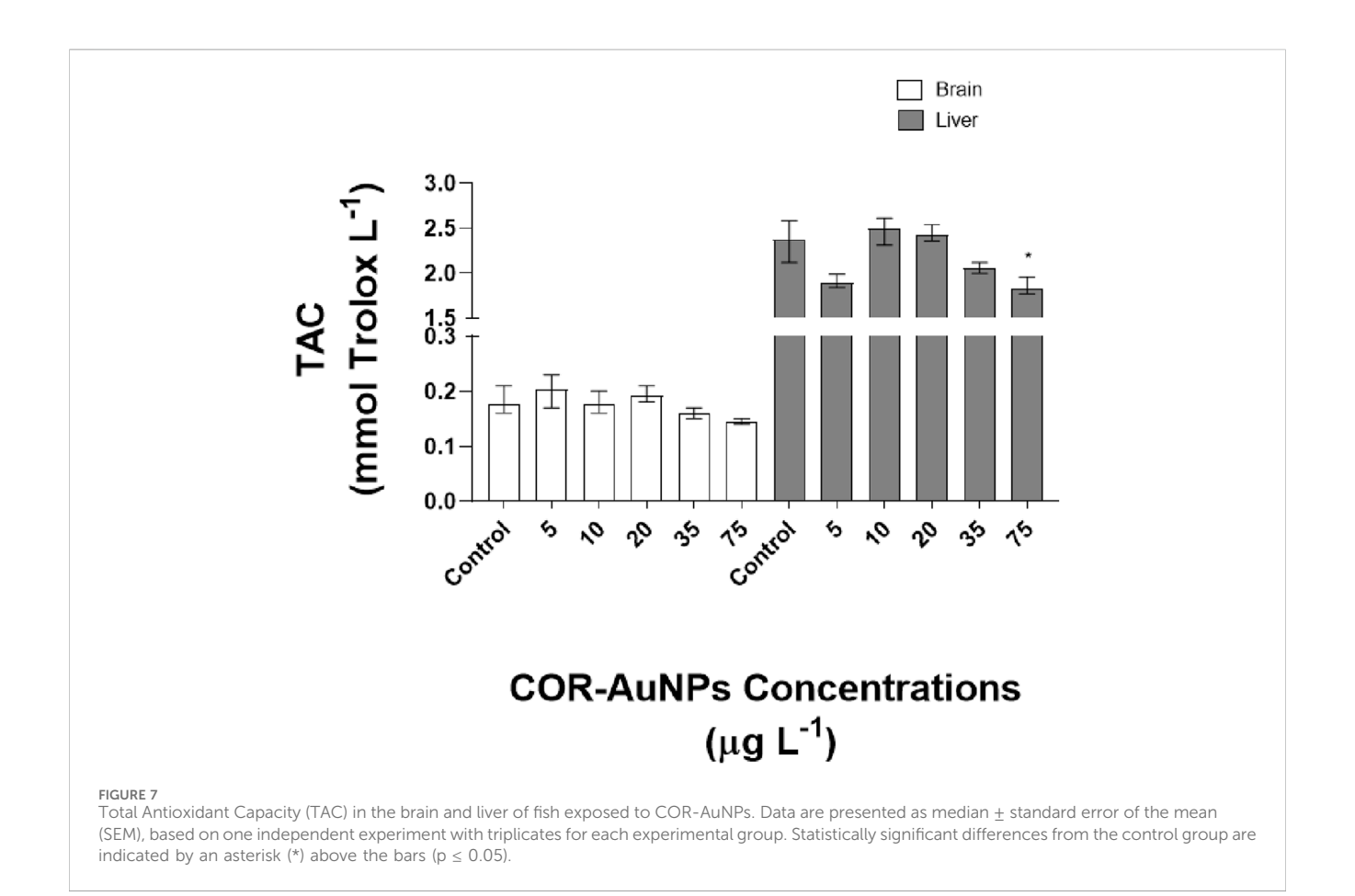
showed values similar to those of the control group (Figure 7). Although this reduction may suggest a potential disturbance in antioxidant capacity at elevated exposure levels, the absence of consistent alterations across other oxidative stress biomarkers limits definitive conclusions. Therefore, when considered in the broader context of this study, the findings do not indicate a pronounced oxidative challenge or impairment of the antioxidant defense system induced by COR-AuNPs.

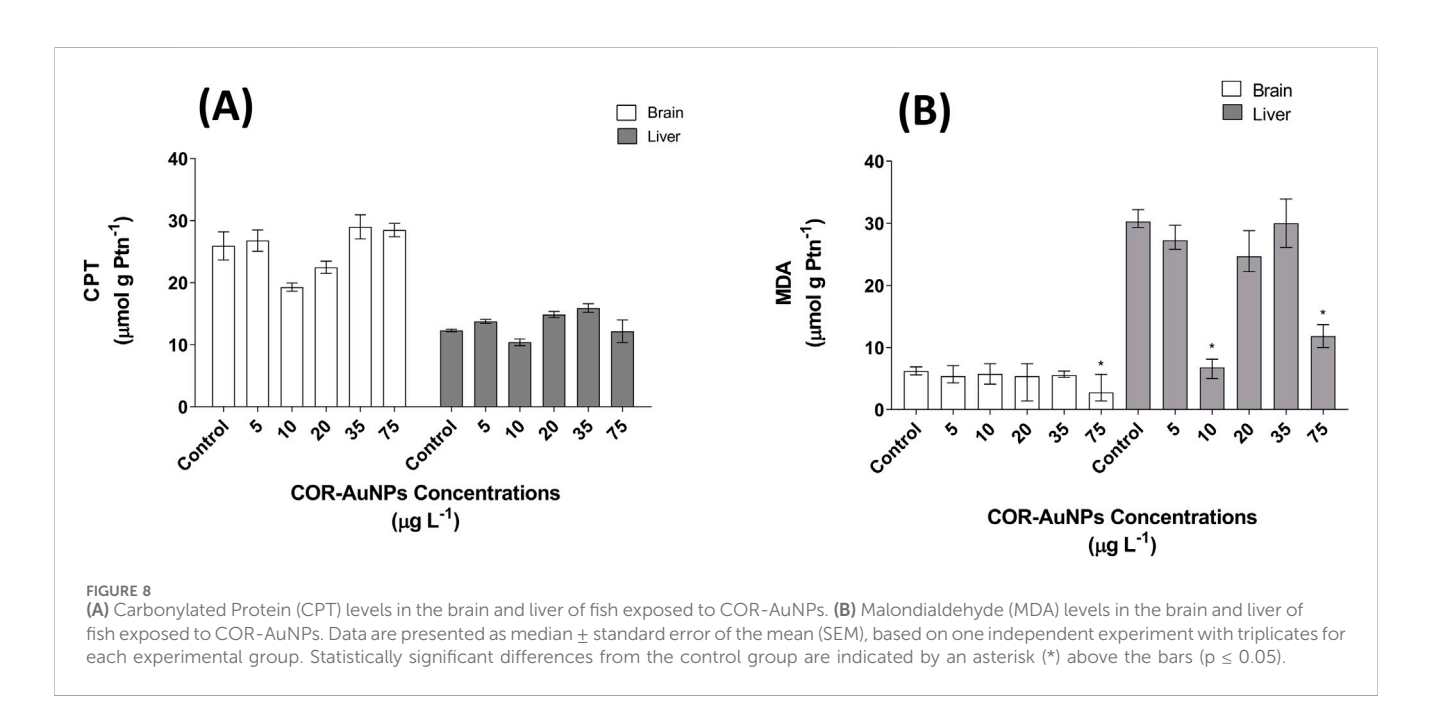
## 3.3.2 Oxidative damage indicative biomarkers - CPT and MDA

The levels of Carbonylated Protein (CPT) and malondialdehyde (MDA), both recognized as biomarkers indicative of cellular oxidative damage (Gryszczyńska et al., 2017; Tsikas, 2017), were evaluated to assess their response to different concentrations of COR-AuNPs. The analysis revealed no significant changes in CPT levels in either the brain or liver across the concentrations tested (Figure 8A). Conversely, a significant reduction in MDA levels was observed in the brain at a concentration of 75 µg.L<sup>-1</sup>. In the liver, MDA levels remained stable at most concentrations, with significant decreases occurring at 10 and 75 µg.L<sup>-1</sup> (Figure 8B), suggesting a potential neuroprotective effect of COR-AuNPs against lipid peroxidation. The present findings are consistent with a prior report indicating that the Turkevich methodsynthesized AuNPs can exert a protective effect on the zebrafish nervous system during co-exposure with ethanol, thereby mitigating the solvent-induced increase in SOD, CAT, and acetylcholinesterase activity (Torres et al., 2021). Additionally, treatment with COR-AuNPs has been documented to markedly diminish the levels of SOD, CAT, xanthine oxidase (XO), GSH, and lipid peroxidation products in the brains of fish exposed to bacterial lipopolysaccharides (LPS) (Sadhukhan et al., 2022). Another study that employed zebrafish cells corroborated these findings by demonstrating that the integration of AuNPs synthesized via a chemical route into a graphene matrix with sizes in the range of a few microns decreases its toxicity, oxidative stress, and aggregation, thereby enhancing the stability of these nanomaterials in biological systems after exposure to 1, 50, and 100 μg mL<sup>-1</sup>. Notably, the highest concentration exhibited a significant reduction compared to AuNPs alone and the graphene oxide-AuNPs hybrid material (Ibrahim et al., 2025).

#### 3.3.3 Genotoxicity

According to the comet assay results, no evidence of DNA damage was observed at any of the tested concentrations of COR-AuNPs, considering regularly previous negative control of organisms not exposed to any contaminants, and positive exposed to methylmethanesulfonate (MMS) at a concentration of 0.4 mM and 0.8 mM (Supplementary Figure S1 on Supplementary Material). This absence of effect was demonstrated by the stable DNA fragmentation levels in the blood cells of the exposed animals, with no increase in Olive Tail Moment (Figure 9A), which reflects the extent of the damage, (Kumaravel et al., 2009), or in tail damage percentage (Figure 9B). These findings are consistent with a previous study (Ramachandran et al., 2018), which also reported no genotoxicity in adult zebrafish from biologically synthesized AuNPs with size and concentration in the range of 30 nm, and 9.7-58.2 mg.L<sup>-1</sup> respectively, using the micronucleus assay. It is notable that the capacity of these nanoparticles to release CO may also contribute to the lack of genetic toxicity, as CO has

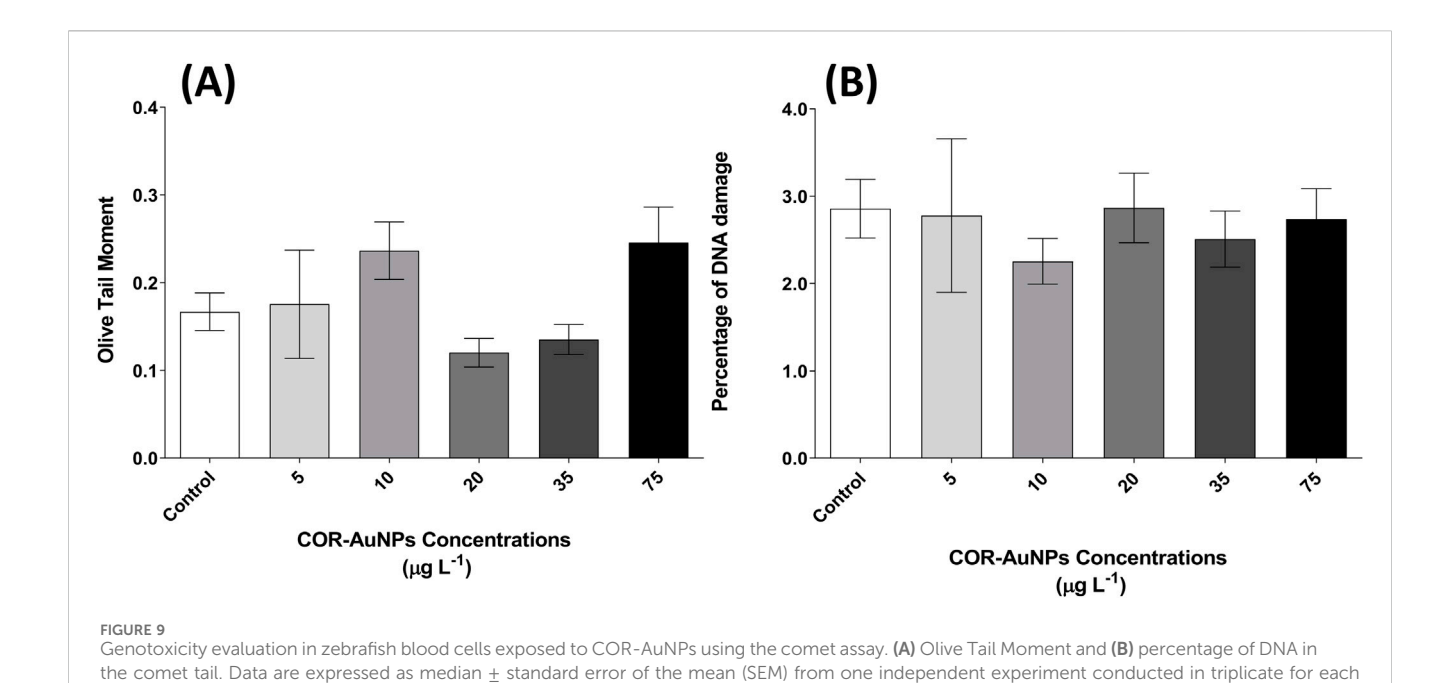




been demonstrated to exert a protective effect on DNA in cells (Juszczak et al., 2020).

The COR-AuNPs synthesized in this study demonstrated a well-defined spherical morphology and maintained high colloidal

stability throughout the experimental period. Our findings reinforce the biocompatibility of these nanoparticles, as no cytotoxic effects were observed in the ECFCs and SaOS-2 cells at none of the concentrations used. Moreover, COR-AuNPs did not



experimental group. No statistically significant differences were observed compared to the control group at any tested concentration. Statistically

induce genotoxicity at any of the tested concentrations. The stability of DNA fragmentation levels in the blood cells of exposed animals confirms the absence of detectable genetic damage under the experimental conditions. The remarkable findings regarding biocompatibility and low toxicity in the biological assays of lasersynthesized COR-AuNPs in cells and in the zebrafish accessed in this work can be related to the synthesis procedure (Tahir et al., 2024), the absence of toxic solvents, with use of solely light-matter interaction, as well as the surrounding atmosphere, inducing the CO<sub>2</sub>RR (Tahir et al., 2024), resulting in the production of COR-AuNPs and organometallic gold based clusters rich in carboxylic acids. Since CO can be used as a protective agent (Ryter et al., 2018), it could be a contributing factor to the stability of oxidative stress biomarkers, absence of significant protein damage, potential neuroprotective effects and lack of genotoxicity, highlighting the safety profile of these nanoparticles. Despite their extensive potential for application in biomedicine, including the delivery of pharmaceuticals (Abu-Dief et al., 2021), antineoplastic therapy (Kumar et al., 2012), antimicrobial action (Li et al., 2014), nanosensors (Hou et al., 2023), and disease diagnostics (Mieszawska et al., 2013), COR-AuNPs hold great promise for

significant differences, when present, are indicated by an asterisk (\*) (p  $\leq$  0.05)

#### 3.4 Literature comparison

The application of metallic nanostructures in biological models (cells and animals) has generated a substantial body of literature, often with conflicting findings due to variations in synthesis methods and experimental models. The use of different concentration ranges in *in vitro* and *in vivo* assays reflects model-specific sensitivities and endpoints. Furthermore, it is

future clinical and technological advancements (Milan et al., 2022).

essential to consider the physicochemical properties of the nanoparticles, which are inherently determined by the synthesis method. Table 1 provides a direct comparison between the synthesis methods used in prior studies and the current approach.

PLA was chosen for this study due to its unique synthesis process, which does not require the use of reagents or surfactants. This distinguishes it from other chemical methods, such as the Brust–Schiffrin protocol (Brust et al., 1994), or ionic liquid-based syntheses (Kim et al., 2004), which do require the use of these substances. These methods still require complex purification to remove residual chemicals, in contrast to the relatively uncomplicated process involved in PLA synthesis.

In comparison with biologically mediated synthesis routes, PLA offers superior reproducibility and better control over key synthesis parameters, including particle size distribution, morphology, and chemical composition. This is particularly especially pronounced in the context of biogenic approaches, which frequently yield nanoparticle formulations that are characterized high polydispersity, a broad spectrum of morphological variants, and inconsistent surface chemistry. For instance, Noruzi et al. (2011) and Shankar et al. (2004) reported the formation of heterogeneous mixtures of gold nanostructures when using biological extracts as reducing and capping agents.

Conversely, laser ablation in liquids facilitates the direct synthesis of nanoparticles in a pristine environment, circumventing the introduction of extraneous contaminants and ensuring greater batch consistency, a prerequisite for biomedical and toxicological investigations.

Furthermore, the physical and chemical characteristics of the nanostructure have been demonstrated to exert a substantial influence on its biological response when exposed to cells or organisms. It has been observed that surface chemistry plays a pivotal role in determining the biological effects of AuNPs. Studies on cellular responses has shown that commonly used stabilizers, such as

TABLE 1 Comparison of different synthesis methods for AuNPs, highlighting key characteristics, limitations, and implications for biological studies. The table critically evaluates chemical, ionic liquid-based, biogenic, and pulsed laser ablation in liquid (PLA) approaches in terms of synthesis yield, and reproducibility.

Synthesis method	Key characteristics	Limitations	Implications for biological studies	References
Chemical (e.g., Brust–Schiffrin)	High synthesis yield; relatively good control over size and morphology	Use of toxic organic solvents and reducing agents (e.g., toluene); extensive purification required	Residual contaminants may interfere with bioassays; reduced biocompatibility	Brust et al. (1994)
Ionic Liquid-based	Greener approach; potential for colloidal stability without conventional surfactants	High cost; potential toxicity of residual salts; limited scalability	Requires toxicity assessment of residual components; limited reproducibility	Kim et al. (2004)
Biogenic (plant/ microbe)	Environmentally friendly; does not require toxic reagents	High polydispersity; limited control over morphology and surface chemistry	Batch-to-batch variability; standardization challenges; risk of biological interference	Shankar et al. (2004), Noruzi et al. (2011)
PLA	Possibility to control surface chemistry of the AuNPs by CO <sub>2</sub> RR; high chemical purity of the core of the NPs; environmentally friendly; does not require toxic reagents	Requires specialized equipment (laser source); lower yield compared to chemical methods	Lowers risk of interference agents; excellent biocompatibility; suitable for biomedical and toxicological applications	Del Rosso et al. (2018), Tahir et al. (2024)

citrate, exhibit negligible toxicity in most cases (Connor et al., 2005; Mironava et al., 2010; Tsai et al., 2013), whereas charged surfactants, particularly those with a positive charge, significantly reduce biocompatibility (Schaeublin et al., 2011). For instance, AuNPs functionalized with CTAB (cetyltrimethylammonium bromide) exhibited higher levels of cellular toxicity in comparison to gold nanorods (AuNRs) in both the Human Dermal Fibroblast and U87 cell lines (Bhamidipati and Fabris, 2017). Furthermore, when CTAB-stabilized AuNRs were exposed to HeLa cells, they exhibited severe toxicity, which was mitigated by replacing the surfactant (Mallick et al., 2013). These findings underscore the dominant role of surface ligands and charge in modulating the biocompatibility of AuNPs.

A comparable trend is evident in zebrafish models, where charged surfactants have been associated with augmented toxicity (Truong et al., 2013). The morphology of AuNPs has been demonstrated to play a significant role in their toxicological profile, particularly at *in vivo* models. In zebrafish, exposure to non-spheroidal nanoparticles resulted in a more pronounced toxic response compared to exposure to spherical particles (Patibandla et al., 2018; Souza et al., 2021). While analogous patterns are discerned in cell models, *in vivo* systems manifest a heightened sensitivity to structural disparities. A number of studies have suggested that AuNPs may exert neuroprotective effects, while others have reported embryotoxicity, including morphological abnormalities and impaired development (Patibandla et al., 2018; Verma et al., 2018; Torres et al., 2021). These findings suggest that nanoparticle shape can significantly influence biological interactions, especially during early developmental stages.

The impact of particle size on the toxicity of AuNPs is a complex matter, as there is a divergence of opinions on the subject. Some evidence has suggested that larger nanoparticles induce greater cytotoxic effects (Mironava et al., 2010), while others have suggested that smaller nanoparticles exhibit higher toxicity due to their greater surface area and reactivity (Broda et al., 2016). These discrepancies underscore the intricacy of size-dependent effects and the impact of confounding variables, such as surface chemistry, agglomeration state and synthesis method. Despite the presence of conflicting findings regarding morphology and size, a clear and consistent trend across studies is the dose-dependent increase in cytotoxic effects. It has been observed that elevated concentrations of AuNPs frequently correlate with augmented toxicity, both cellular and systemic (Connor et al.,

2005; Mironava et al., 2010; Schaeublin et al., 2011; Tsai et al., 2013; Broda et al., 2016; Bhamidipati and Fabris, 2017). In zebrafish, for instance, exposure to AuNP resulted in both dose-dependent toxicity and tissue-specific bioaccumulation in the brain, muscles, gills, and gastrointestinal tract, evaluated over a 60-day period (Geffroy et al., 2012). This accumulation may be associated with long-term toxic effects, including modulation in the expression of genes related to DNA repair and detoxification pathways (Geffroy et al., 2012; Dedeh et al., 2015). Consequently, further studies with the COR-AuNPs synthesized in the present work are warranted to evaluate longer exposure periods and potential cumulative effects.

Another relevant aspect concerns the selection of sublethal endpoins. Torres et al. (2021); Sadhukhan et al. (2022) reported that AuNPs can modulate endogenous antioxidant defenses and influence the activity of key enzymes in zebrafish. Importantly, (Torres et al., 2021), observed that these parameters returned to baseline after exposure, indicating a transient and reversible sublethal biological response (Torres et al., 2021). In line with these findings, our study also focused on sublethal endpoints, evaluating sensitive oxidative stress biomarkers and early indicators of cellular damage, including lipid peroxidation (MDA), protein carbonylation (PTC), and DNA damage (comet assay), and found no significant alterations following acute exposure to COR-AuNPs.

This study offers a significant advancement in the field by assessing the toxicity of gold nanoparticles produced by pulsed laser ablation, enriched with oxocarbons, in zebrafish. Notably, the synthesis approach employed in this research is devoid of chemical contaminants, a notable feature that enhances the study's rigor and reliability. In the literature, Gong et al. (2016) reported that cobalt-based CORMs did not induce significant toxicity in zebrafish embryos at concentrations below 1.0  $\mu M$  (equivalent to about 60.0  $\mu g \cdot L^{-1}$  of Co) Gong et al. (2016). Comparatively, in the present study, COR-AuNPs were tested at concentrations ranging from 5 to 75  $\mu g \cdot L^{-1}$ , without causing mortality or significant alterations in oxidative stress and genotoxicity biomarkers. These results reinforce that CO-releasing nanomaterials, when properly stabilized and free of toxic ligands, may exhibit a safe profile at concentration ranges similar to those previously established for cobalt-based CORMs.

Therefore, the present study demonstrates that COR-AuNPs produced by pulsed laser ablation exhibit high biocompatibility in

zebrafish, with no significant acute toxicity or sublethal effects observed at the concentrations that were tested. These results are consistent with previous findings for cobalt-based CORMs and highlight the critical influence of synthesis method, surface chemistry, and particle size on the biological responses to metallic nanoparticles. Furthermore, subsequent studies should encompass conventional gold nanoparticles devoid of CO-release properties to distinguish the effects attributable to CO from those of the nanoparticle core.

## 4 Conclusion

This study provides consistent evidence of angiogenic responses of the COR-AuNPs to treated ECFCs. The safety profile of the lasersynthesized COR-AuNPs was thoroughly demonstrated, showing low cytotoxicity to human cells, limited effects on oxidative stress biomarkers, and absence of genotoxicity in zebrafish, a well-established model for human-related toxicological and biomedical research. These findings underscore the potential of COR-AuNPs for biomedical applications, particularly in light their clean synthesis route, free from surfactants and undesired residual ligands, which distinguishes them from conventionally produced AuNPs. It is imperative to note, however, that the biological behavior of the COR-AuNPs is intimately associated with their physicochemical characteristics and the experimental parameters of the synthesis method, which have the potential to vary, for instance, in terms of their CO content. Consequently, while the results obtained herein provide valuable insights into the biocompatibility of this specific nanomaterial, further studies are necessary to explore its long-term effects, potential for bioaccumulation, and responses under varying physiological conditions, thereby supporting the safe and effective use of COR-AuNPs in future biomedical applications.

## Data availability statement

The raw data supporting the conclusions of this article will be made available by the authors, without undue reservation.

## **Ethics statement**

Ethical approval was not required for the studies on humans in accordance with the local legislation and institutional requirements because only commercially available established cell lines were used. The animal study was approved by Animal Use Ethics Committee of the Oswaldo Cruz Institute (CEUA IOC) - Protocol 035/2022 and license L-001/2023-A1, valid until 2026. The study was conducted in accordance with the local legislation and institutional requirements.

### **Author contributions**

TG: Writing – review and editing, Methodology, Investigation, Data curation, Writing – original draft, Visualization. GC: Visualization, Data curation, Investigation, Methodology, Writing – original draft, Writing – review and editing. MG: Methodology, Investigation, Writing – review and editing. GA: Methodology, Writing – review

and editing. LB: Data curation, Methodology, Validation, Funding acquisition, Writing - original draft, Investigation, Writing - review and editing, Resources, Formal Analysis. LC: Validation, Methodology, Writing - review and editing, Data curation, Investigation. LS: Methodology, Writing - review and editing, Resources. SS: Writing - review and editing, Formal Analysis, Methodology, Data curation. DC: Investigation, Methodology, Writing - review and editing. FC: Supervision, Writing - review and editing. AL: Writing review and editing, Data curation, Methodology, Supervision, Conceptualization, Formal analysis, Investigation, Resources, Software. CA: Investigation, Methodology, Writing - Review and editing. EF: Investigation, Methodology, Writing - Review and editing. AC: Writing review and editing, Data curation, Methodology, Supervision, Conceptualization, Formal analysis, Investigation, Resources, Project administration, Visualization. FM: Writing - review and editing, Data curation, Methodology, Supervision, Conceptualization, Formal analysis, Investigation, Resources, Project administration, Visualization. TD: Supervision, Writing - original draft, Funding acquisition, Writing - review and editing, Conceptualization, Resources. ES: Writing - review and editing, Conceptualization, Writing - original draft, Supervision, Funding acquisition, Resources, Validation, Project administration.

## **Funding**

The author(s) declare that financial support was received for the research and/or publication of this article. The authors would like to thank the Higher Education Personnel (Coordination for the Improvement of Higher Education Personnel–CAPES), project n° 001/2021. EMS is grateful for the "Jovem Cientista do Nosso Estado" a scholarship awarded by the Research Support Foundation of the State of Rio de Janeiro (FAPERJ - Project E-21/201.271/2021),National Council for Scientific and Technological Development (CNPq 304571/2021–0), and support from Carlos Chagas Filho Foundation for Research Support of the State of Rio de Janeiro (FAPERJ) in the FAPERJ NOTA 10, and in the project FAPERJ E-26/10.000981/2019, Rede NanoSaúde/FAPERJ. This work was financially supported by Associazione Italiana Ricerca sulCancro (AIRC) grant IG 2020 N. 24,381, by Tuscany Region (Call on HealthBando Ricerca Salute 2018 through Project "THERMINATOR").

## Acknowledgments

The authors express their gratitude to Renata Jurema Medeiros and her team for providing the facilities for animal experimentation at the National Institute for Quality Control in Health (INCQS) of the Oswaldo Cruz Foundation (FIOCRUZ). And Wanderson de Souza and Diego Wiechers (both from Inmetro) in pre-tests of MTS *in vitro* test.

#### Conflict of interest

The authors declare that the research was conducted in the absence of any commercial or financial relationships that could be construed as a potential conflict of interest.

The author(s) declared that they were an editorial board member of Frontiers, at the time of submission. This had no impact on the peer review process and the final decision.

#### Generative Al statement

The author(s) declare that no Generative AI was used in the creation of this manuscript.

Any alternative text (alt text) provided alongside figures in this article has been generated by Frontiers with the support of artificial intelligence and reasonable efforts have been made to ensure accuracy, including review by the authors wherever possible. If you identify any issues, please contact us.

#### References

Abbasi, R., Shineh, G., Mobaraki, M., Doughty, S., and Tayebi, L. (2023). Structural parameters of nanoparticles affecting their toxicity for biomedical applications: a review. *J. Nanoparticle Res.* 25, 43. doi:10.1007/s11051-023-05690-w

ABNT NBR (2022). ABNT NBR 15088:2011 - aquatic ecotoxicology - acute toxicity - test with fish. Brazil: NORMAS BRASILEIRAS.

Abu-Dief, A. M., Salaheldeen, M., and El-Dabea, T. (2021). Recent advances in development of gold nanoparticles for drug delivery systems. *J. Mod. Nanotechnol.* 1. doi:10.53964/jmn.2021001

Aebi, H. (1984). Catalase in vitro. Methods Enzymol. 105, 121–126. doi:10.1016/S0076-6879(84)05016-3

Al-Huseini, L. M. A., Aw Yeang, H. X., Hamdam, J. M., Sethu, S., Alhumeed, N., Wong, W., et al. (2014). Heme Oxygenase-1 regulates dendritic cell function through modulation of p38 MAPK-CREB/ATF1 signaling. *J. Biol. Chem.* 289, 16442–16451. doi:10.1074/jbc.M113.532069

Anwar, S., Alrumaihi, F., Sarwar, T., Babiker, A. Y., Khan, A. A., Prabhu, S. V., et al. (2024). Exploring therapeutic potential of catalase: strategies in disease prevention and management. *Biomolecules* 14, 697. doi:10.3390/biom14060697

Araujo, G. de F., Soares, L. O. S., Junior, S. F. S., Barreto de Carvalho, L. V., Rocha, R. C. C., Saint'Pierre, T., et al. (2022). Oxidative stress and metal homeostasis alterations in *Danio rerio* (zebrafish) under single and combined carbamazepine, acetamiprid and cadmium exposures. *Aquat. Toxicol.* 245, 106122. doi:10.1016/j. aquatox.2022.106122

Armanetti, P., Chillà, A., Margheri, F., Biagioni, A., Menichetti, L., Margheri, G., et al. (2021). Enhanced antitumoral activity and photoacoustic imaging properties of AuNP-Enriched endothelial colony forming cells on melanoma. *Adv. Sci.* 8, 2001175. doi:10. 1002/advs.202001175

Arunachalam, M., Raja, M., Vijayakumar, C., Malaiammal, P., and Mayden, R. L. (2013). Natural history of zebrafish (*Danio rerio*) in India. *Zebrafish* 10, 1–14. doi:10. 1089/zeb.2012.0803

Bagul, A., Hosgood, S. A., Kaushik, M., and Nicholson, M. L. (2008). Carbon monoxide protects against ischemia-reperfusion injury in an experimental model of controlled nonheartbeating donor kidney. *Transplantation* 85, 576–581. doi:10.1097/TP.0b013e318160516a

Balasubramanian, S. K., Yang, L., Yung, L.-Y. L., Ong, C.-N., Ong, W.-Y., and Yu, L. E. (2010). Characterization, purification, and stability of gold nanoparticles. *Biomaterials* 31, 9023–9030. doi:10.1016/j.biomaterials.2010.08.012

Bannenberg, G. L., and Vieira, H. L. A. (2009). Therapeutic applications of the gaseous mediators carbon monoxide and hydrogen sulfide. *Expert Opin. Ther. Pat.* 19, 663–682. doi:10.1517/13543770902858824

Barreto, A., Luis, L. G., Pinto, E., Almeida, A., Paíga, P., Santos, L. H. M. L. M., et al. (2019). Effects and bioaccumulation of gold nanoparticles in the gilthead seabream (*Sparus aurata*) – single and combined exposures with gemfibrozil. *Chemosphere* 215, 248–260. doi:10.1016/j.chemosphere.2018.09.175

Bhamidipati, M., and Fabris, L. (2017). Multiparametric assessment of gold nanoparticle cytotoxicity in cancerous and healthy cells: the role of size, shape, and surface chemistry. *Bioconjug. Chem.* 28, 449–460. doi:10.1021/acs.bioconjchem.

Borski, R. J., and Hodson, R. G. (2003). Fish research and the institutional animal care and use committee. *ILAR J.* 44, 286–294. doi:10.1093/ilar.44.4.286

Briggs, J. P. (2002). The zebrafish: a new model organism for integrative physiology. Am. J. Physiol. Integr. Comp. Physiol. 282, R3–R9. doi:10.1152/ajpregu.00589.2001

#### Publisher's note

All claims expressed in this article are solely those of the authors and do not necessarily represent those of their affiliated organizations, or those of the publisher, the editors and the reviewers. Any product that may be evaluated in this article, or claim that may be made by its manufacturer, is not guaranteed or endorsed by the publisher.

## Supplementary material

The Supplementary Material for this article can be found online at: https://www.frontiersin.org/articles/10.3389/fbioe.2025.1594693/full#supplementary-material

Broda, J., Setzler, J., Leifert, A., Steitz, J., Benz, R., Simon, U., et al. (2016). Ligand-lipid and ligand-core affinity control the interaction of gold nanoparticles with artificial lipid bilayers and cell membranes. *Nanomedicine Nanotechnol. Biol. Med.* 12, 1409–1419. doi:10.1016/j.nano.2015.12.384

Browning, L. M., Lee, K. J., Huang, T., Nallathamby, P. D., Lowman, J. E., and Nancy Xu, X.-H. (2009). Random walk of single gold nanoparticles in zebrafish embryos leading to stochastic toxic effects on embryonic developments. *Nanoscale* 1, 138. doi:10. 1039/b9nr00053d

Brust, M., Walker, M., Bethell, D., Schiffrin, D. J., and Whyman, R. (1994). Synthesis of thiol-derivatised gold nanoparticles in a two-phase liquid-liquid system. *J. Chem. Soc. Chem. Commun.* 0, 801–802. doi:10.1039/C39940000801

Cabuzu, D., Cirja, A., Puiu, R., and Grumezescu, A. (2015). Biomedical applications of gold nanoparticles. *Curr. Top. Med. Chem.* 15, 1605–1613. doi:10.2174/1568026615666150414144750

Chai, Y.-C., and Mieyal, J. J. (2023). Glutathione and glutaredoxin—key players in cellular redox homeostasis and signaling. *Antioxidants* 12, 1553. doi:10.3390/antiox12081553

Chen, B., Guo, L., Fan, C., Bolisetty, S., Joseph, R., Wright, M. M., et al. (2009). Carbon monoxide rescues heme Oxygenase-1-Deficient mice from arterial thrombosis in allogeneic aortic transplantation. *Am. J. Pathol.* 175, 422–429. doi:10.2353/ajpath. 2009.081033

Chen, H., Dai, Y., Cui, J., Yin, X., Feng, W., lv, M., et al. (2021). Carbon monoxide releasing Molecule-3 enhances osteogenic differentiation of human periodontal ligament stem cells by carbon monoxide release. *Drug Des. devel. Ther.* 15, 1691–1704. doi:10.2147/DDDT.S300356

Cheng, J., and Hu, J. (2021). Recent advances on carbon monoxide releasing molecules for antibacterial applications. ChemMedChem~16,~3628-3634.~doi:10.1002/cmdc.202100555

Chillà, A., Anceschi, C., Scavone, F., Martinelli, S., Ruzzolini, J., Frediani, E., et al. (2025). Sparking angiogenesis by carbon monoxide-rich gold nanoparticles obtained by pulsed laser driven CO<sub>2</sub> reduction reaction. *J. Nanobiotechnol.* 23, 590. doi:10.1186/s12951-025-03680-9

Choi, H.-I., Zeb, A., Kim, M.-S., Rana, I., Khan, N., Qureshi, O. S., et al. (2022). Controlled therapeutic delivery of CO from carbon monoxide-releasing molecules (CORMs). *J. Control. Release* 350, 652–667. doi:10.1016/j.jconrel.2022.08.055

Chu, L. M., Shaefi, S., Byrne, J. D., Alves de Souza, R. W., and Otterbein, L. E. (2021). Carbon monoxide and a change of heart. *Redox Biol.* 48, 102183. doi:10.1016/j.redox. 2021.102183

Clark, J. E., Naughton, P., Shurey, S., Green, C. J., Johnson, T. R., Mann, B. E., et al. (2003). Cardioprotective actions by a water-soluble carbon monoxide-releasing molecule. *Circ. Res.* 93, e2–e8. doi:10.1161/01.RES.0000084381.86567.08

CONCEA - Conselho Nacional de Controle de Experimentação Animal (2015). Diretriz da prática de eutanásia do CONCEA. *Brasilia*.

Connor, E. E., Mwamuka, J., Gole, A., Murphy, C. J., and Wyatt, M. D. (2005). Gold nanoparticles are taken up by human cells but do not cause acute cytotoxicity. Small 1, 325-327. doi:10.1002/smll.200400093

Crook, S. H., Mann, B. E., Meijer, A. J. H. M., Adams, H., Sawle, P., Scapens, D., et al. (2011). [Mn(CO)4{S2CNMe(CH2CO2H)}], a new water-soluble CO-releasing molecule. *Dalt. Trans.* 40, 4230. doi:10.1039/c1dt10125k

Dalle Carbonare, L., Cominacini, M., Trabetti, E., Bombieri, C., Pessoa, J., Romanelli, M. G., et al. (2025). The bone microenvironment: new insights into the role of stem cells

and cell communication in bone regeneration. Stem Cell Res. Ther. 16, 169. doi:10.1186/s13287-025-04288-4

Dedeh, A., Ciutat, A., Treguer-Delapierre, M., and Bourdineaud, J.-P. (2015). Impact of gold nanoparticles on zebrafish exposed to a spiked sediment. *Nanotoxicology* 9, 71–80. doi:10.3109/17435390.2014.889238

Del Rosso, T., Rey, N. A., Rosado, T., Landi, S., Larrude, D. G., Romani, E. C., et al. (2016). Synthesis of oxocarbon-encapsulated gold nanoparticles with blue-shifted localized surface plasmon resonance by pulsed laser ablation in water with CO  $_2$  absorbers. Nanotechnology 27, 255602. doi:10.1088/0957-4484/27/25/255602

Del Rosso, T., Louro, S. R. W., Deepak, F. L., Romani, E. C., Zaman, Q., Tahir, et al. (2018). Biocompatible Au@Carbynoid/Pluronic-F127 nanocomposites synthesized by pulsed laser ablation assisted CO2 recycling. *Appl. Surf. Sci.* 441, 347–355. doi:10.1016/j. apsusc.2018.02.007

Diomede, F., Marconi, G. D., Fonticoli, L., Pizzicanella, J., Merciaro, I., Bramanti, P., et al. (2020). Functional relationship between osteogenesis and angiogenesis in tissue regeneration. *Int. J. Mol. Sci.* 21, 3242. doi:10.3390/ijms21093242

Dulak, J., Deshane, J., Jozkowicz, A., and Agarwal, A. (2008). Heme Oxygenase-1 and carbon monoxide in vascular pathobiology. *Circulation* 117, 231–241. doi:10.1161/CIRCULATIONAHA.107.698316

Elagin, V. V., Sergeeva, E. A., Bugrova, M. L., Ignatova, N. I., Yuzhakova, D. V., Denisov, N. N., et al. (2014). Selection of stabilizing agents to provide effective penetration of gold nanoparticles into cells. *Photonics Lasers Med.* 3. doi:10.1515/plm-2014-0016

Fayad-Kobeissi, S., Ratovonantenaina, J., Dabiré, H., Wilson, J. L., Rodriguez, A. M., Berdeaux, A., et al. (2016). Vascular and angiogenic activities of CORM-401, an oxidant-sensitive CO-releasing molecule. *Biochem. Pharmacol.* 102, 64–77. doi:10. 1016/j.bcp.2015.12.014

Forman, H. J., Zhang, H., and Rinna, A. (2009). Glutathione: overview of its protective roles, measurement, and biosynthesis. *Mol. Asp. Med.* 30, 1–12. doi:10.1016/j.mam. 2008.08.006

Ganong, W. (1995). Review of medical physiology, dynamics of blood and lymph flow. Upper Saddle River: Lange Medical Publication.

Ge, W., Yan, S., Wang, J., Zhu, L., Chen, A., and Wang, J. (2015). Oxidative stress and DNA damage induced by imidacloprid in zebrafish (*Danio rerio*). *J. Agric. Food Chem.* 63, 1856–1862. doi:10.1021/jf504895h

Geffroy, B., Ladhar, C., Cambier, S., Treguer-Delapierre, M., Brèthes, D., and Bourdineaud, J.-P. (2012). Impact of dietary gold nanoparticles in zebrafish at very low contamination pressure: the role of size, concentration and exposure time. *Nanotoxicology* 6, 144–160. doi:10.3109/17435390.2011.562328

Gomes, T. B., Fernandes Sales Junior, S., Saint'Pierre, T. D., Correia, F. V., Hauser-Davis, R. A., and Saggioro, E. M. (2019). Sublethal psychotropic pharmaceutical effects on the model organism *Danio rerio*: oxidative stress and metal dishomeostasis. *Ecotoxicol. Environ. Saf.* 171, 781–789. doi:10.1016/j.ecoenv.2019.01.041

Gong, Y., Zhang, T., Li, M., Xi, N., Zheng, Y., Zhao, Q., et al. (2016). Toxicity, bio-distribution and metabolism of CO-releasing molecules based on cobalt. *Free Radic. Biol. Med.* 97, 362–374. doi:10.1016/j.freeradbiomed.2016.06.029

Gryszczyńska, B., Formanowicz, D., Budzyń, M., Wanic-Kossowska, M., Pawliczak, E., Formanowicz, P., et al. (2017). Advanced oxidation protein products and carbonylated proteins as biomarkers of oxidative stress in selected atherosclerosis-mediated diseases. *Biomed. Res. Int.* 2017, 1–9. doi:10.1155/2017/4975264

Habig, W. H., Pabst, M. J., and Jakoby, W. B. (1974). Glutathione S-Transferases. J. Biol. Chem. 249, 7130–7139. doi:10.1016/S0021-9258(19)42083-8

Haque, E., and Ward, A. C. (2018). Zebrafish as a model to evaluate nanoparticle toxicity. *Nanomaterials* 8, 561. doi:10.3390/nano8070561

Herrmann, W. A. (1990). 100 years of metal carbonyls: a serendipitous chemical discovery of major scientific and industrial impact. *J. Organomet. Chem.* 383, 21–44. doi:10.1016/0022-328X(90)85120-N

Horie, M., and Tabei, Y. (2021). Role of oxidative stress in nanoparticles toxicity. *Free Radic. Res.* 55, 331–342. doi:10.1080/10715762.2020.1859108

Hou, S., Ma, J., Cheng, Y., Wang, Z., and Yan, Y. (2023). Overview—Gold nanoparticles-based sensitive nanosensors in mycotoxins detection. *Crit. Rev. Food Sci. Nutr.* 63, 11734–11749. doi:10.1080/10408398.2022.2095973

Howe, K., Clark, M. D., Torroja, C. F., Torrance, J., Berthelot, C., Muffato, M., et al. (2013). The zebrafish reference genome sequence and its relationship to the human genome. *Nature* 496, 498–503. doi:10.1038/nature12111

Ibrahim, B., Akere, T. H., Dhumal, P., Valsami-Jones, E., and Chakraborty, S. (2025). Designing safer nanohybrids: stability and ecotoxicological assessment of graphene oxide-gold nanoparticle hybrids in embryonic zebrafish. *Environ. Sci. Nano.* 12, 1965–1978. doi:10.1039/D4EN01173B

Jacquel, A., Herrant, M., Legros, L., Belhacene, N., Luciano, F., Pages, G., et al. (2003). Imatinib induces mitochondria-dependent apoptosis of the Bcr-Abl-positive K562 cell line and its differentiation toward the erythroid lineage 1. FASEB J. 17, 2160–2162. doi:10.1096/fj.03-0322

Jawaid, P., Rehman, M. U., Zhao, Q.-L., Misawa, M., Ishikawa, K., Hori, M., et al. (2020). Small size gold nanoparticles enhance apoptosis-induced by cold atmospheric

plasma via depletion of intracellular GSH and modification of oxidative stress. Cell Death Discov. 6, 83. doi:10.1038/s41420-020-00314-x

Juan, C. A., Pérez de la Lastra, J. M., Plou, F. J., and Pérez-Lebeña, E. (2021). The chemistry of reactive oxygen species (ROS) revisited: outlining their role in biological macromolecules (DNA, lipids and proteins) and induced pathologies. *Int. J. Mol. Sci.* 22, 4642. doi:10.3390/ijms22094642

Juszczak, M., Kluska, M., Wysokiński, D., and Woźniak, K. (2020). DNA damage and antioxidant properties of CORM-2 in normal and cancer cells. *Sci. Rep.* 10, 12200. doi:10.1038/s41598-020-68948-6

Kamstra, J. H., Aleström, P., Kooter, J. M., and Legler, J. (2015). Zebrafish as a model to study the role of DNA methylation in environmental toxicology. *Environ. Sci. Pollut. Res.* 22, 16262–16276. doi:10.1007/s11356-014-3466-7

Kautz, A. C., Kunz, P. C., and Janiak, C. (2016). CO-releasing molecule (CORM) conjugate systems. *Dalt. Trans.* 45, 18045–18063. doi:10.1039/C6DT03515A

Kim, K.-S., Demberelnyamba, D., and Lee, H. (2004). Size-selective synthesis of gold and platinum nanoparticles using novel thiol-functionalized ionic liquids. Langmuir~20, 556–560. doi:10.1021/la0355848

Kneipp, K., Wang, Y., Kneipp, H., Perelman, L. T., Itzkan, I., Dasari, R. R., et al. (1997). Single molecule detection using surface-enhanced raman scattering (SERS). *Phys. Rev. Lett.* 78, 1667–1670. doi:10.1103/PhysRevLett.78.1667

Koramutla, M. K., Negi, M., and Ayele, B. T. (2021). Roles of glutathione in mediating abscisic acid signaling and its regulation of seed dormancy and drought tolerance. Genes (Basel) 12, 1620. doi:10.3390/genes12101620

Krishnamurthy, H. K., Pereira, M., Rajavelu, I., Jayaraman, V., Krishna, K., Wang, T., et al. (2024). Oxidative stress: fundamentals and advances in quantification techniques. *Front. Chem.* 12, 1470458. doi:10.3389/fchem.2024.1470458

Kumar, A., Ma, H., Zhang, X., Huang, K., Jin, S., Liu, J., et al. (2012). Gold nanoparticles functionalized with therapeutic and targeted peptides for cancer treatment. *Biomaterials* 33, 1180–1189. doi:10.1016/j.biomaterials.2011.10.058

Kumaravel, T. S., Vilhar, B., Faux, S. P., and Jha, A. N. (2009). Comet assay measurements: a perspective. *Cell Biol. Toxicol.* 25, 53–64. doi:10.1007/s10565-007-9043-0

Landi, S. (2000). Mammalian class theta GST and differential susceptibility to carcinogens: a review. *Mutat. Res. Mutat. Res.* 463, 247–283. doi:10.1016/S1383-5742(00)00050-8

Li, X., Robinson, S. M., Gupta, A., Saha, K., Jiang, Z., Moyano, D. F., et al. (2014). Functional gold nanoparticles as potent antimicrobial agents against multi-drug-resistant bacteria. *ACS Nano* 8, 10682–10686. doi:10.1021/pn504265

Lim, S. H., Wong, T. W., and Tay, W. X. (2024). Overcoming colloidal nanoparticle aggregation in biological milieu for cancer therapeutic delivery: perspectives of materials and particle design. *Adv. Colloid Interface Sci.* 325, 103094. doi:10.1016/j.cis.2024. 103094

Lowry, O., Rosebrough, N., Farr, A. L., and Randall, R. (1951). Protein measurement with the folin phenol reagent. *J. Biol. Chem.* 193, 265–275. doi:10.1016/S0021-9258(19) 52451-6

Luis, L. G., Barreto, Â., Trindade, T., Soares, A. M. V. M., and Oliveira, M. (2016). Effects of emerging contaminants on neurotransmission and biotransformation in marine organisms — an *in vitro* approach. *Mar. Pollut. Bull.* 106, 236–244. doi:10.1016/j.marpolbul.2016.02.064

Luo, M., Boudier, A., Clarot, I., Maincent, P., Schneider, R., and Leroy, P. (2016). Gold nanoparticles grafted by reduced glutathione with thiol function preservation. *Colloid Interface Sci. Commun.* 14, 8–12. doi:10.1016/j.colcom.2016.07.002

Lushchak, V. I. (2012). Glutathione homeostasis and functions: potential targets for medical interventions. *J. Amino Acids* 2012, 736837. doi:10.1155/2012/736837

Lushchak, V. I., and Storey, K. B. (2021). Oxidative stress concept updated: definitions, classifications, and regulatory pathways implicated. *EXCLI J.* 20, 956–967. doi:10.17179/excli2021-3596

Mahaye, N., Thwala, M., Cowan, D. A., and Musee, N. (2017). Genotoxicity of metal based engineered nanoparticles in aquatic organisms: a review. *Mutat. Res. Mutat. Res.* 773, 134–160. doi:10.1016/j.mrrev.2017.05.004

Mallick, S., Sun, I.-C., Kim, K., and Yi, D. K. (2013). Silica coated gold nanorods for imaging and photo-thermal therapy of cancer cells. *J. Nanosci. Nanotechnol.* 13, 3223–3229. doi:10.1166/jnn.2013.7149

Mansour, A. M., Khaled, R. M., Khaled, E., Ahmed, S. K., Ismael, O. S., Zeinhom, A., et al. (2022). Ruthenium(II) carbon monoxide releasing molecules: structural perspective, antimicrobial and anti-inflammatory properties. *Biochem. Pharmacol.* 199, 114991. doi:10.1016/j.bcp.2022.114991

Margheri, F., Chillà, A., Laurenzana, A., Serrati, S., Mazzanti, B., Saccardi, R., et al. (2011). Endothelial progenitor cell–dependent angiogenesis requires localization of the full-length form of uPAR in caveolae. *Blood* 118, 3743–3755. doi:10.1182/blood-2011-02-338681

Mesquita, C. S., Oliveira, R., Bento, F., Geraldo, D., Rodrigues, J. V., and Marcos, J. C. (2014). Simplified 2,4-dinitrophenylhydrazine spectrophotometric assay for quantification of carbonyls in oxidized proteins. *Anal. Biochem.* 458, 69–71. doi:10. 1016/j.ab.2014.04.034

Meyers, J. R. (2018). Zebrafish: development of a vertebrate model organism. Curr. Protoc. Essent. Lab. Tech. 16, e19. doi:10.1002/cpet.19

Mieszawska, A. J., Mulder, W. J. M., Fayad, Z. A., and Cormode, D. P. (2013). Multifunctional gold nanoparticles for diagnosis and therapy of disease. *Mol. Pharm.* 10, 831–847. doi:10.1021/mp3005885

Milan, J., Niemczyk, K., and Kus-Liśkiewicz, M. (2022). Treasure on the earth—gold nanoparticles and their biomedical applications. *Mater. (Basel)* 15, 3355. doi:10.3390/ma15093355

Mironava, T., Hadjiargyrou, M., Simon, M., Jurukovski, V., and Rafailovich, M. H. (2010). Gold nanoparticles cellular toxicity and recovery: effect of size, concentration and exposure time. *Nanotoxicology* 4, 120–137. doi:10.3109/17435390903471463

Møller, P., Azqueta, A., Boutet-Robinet, E., Koppen, G., Bonassi, S., Milić, M., et al. (2020). Minimum information for reporting on the comet assay (MIRCA): recommendations for describing comet assay procedures and results. *Nat. Protoc.* 15, 3817–3826. doi:10.1038/s41596-020-0398-1

Moore, T., Croy, S., Mallapragada, S., and Pandit, N. (2000). Experimental investigation and mathematical modeling of pluronic  $^{\otimes}$  F127 gel dissolution: drug release in stirred systems. *J. Control. Release* 67, 191–202. doi:10.1016/S0168-3659(00)00215-7

Motterlini, R., and Otterbein, L. E. (2010). The therapeutic potential of carbon monoxide. *Nat. Rev. Drug Discov.* 9, 728–743. doi:10.1038/nrd3228

Motterlini, R., Clark, J. E., Foresti, R., Sarathchandra, P., Mann, B. E., and Green, C. J. (2002). Carbon monoxide-releasing molecules: characterization of biochemical and vascular activities. *Circ. Res.* 90, E17–E24. doi:10.1161/hh0202.104530

Motterlini, R., Sawle, P., Bains, S., Hammad, J., Alberto, R., Foresti, R., et al. (2005). CORM-A1: a new pharmacologically active carbon monoxide-releasing molecule. *FASEB J.* 19, 1–24. doi:10.1096/fj.04-2169fje

Muniz-Miranda, M., Del Rosso, T., Giorgetti, E., Margheri, G., Ghini, G., and Cicchi, S. (2011). Surface-enhanced fluorescence and surface-enhanced Raman scattering of push-pull molecules: sulfur-functionalized 4-amino-7-nitrobenzofurazan adsorbed on Ag and Au nanostructured substrates. *Anal. Bioanal. Chem.* 400, 361–367. doi:10.1007/s00216-011-4732-x

Murphy, C. J., and Jana, N. R. (2002). Controlling the aspect ratio of inorganic nanorods and nanowires. Adv.~Mater.~14, 80-82.~doi:10.1002/1521-4095(20020104)14: 1<80::AID-ADMA80>3.0.CO;2-#

Mutalik, C., Nivedita, Sneka, C., Krisnawati, D. I., Yougbaré, S., Hsu, C.-C., et al. (2024). Zebrafish insights into nanomaterial toxicity: a focused exploration on metallic, metal oxide, semiconductor, and mixed-metal nanoparticles. *Int. J. Mol. Sci.* 25, 1926. doi:10.3390/ijms25031926

Nakao, A., Faleo, G., Shimizu, H., Nakahira, K., Kohmoto, J., Sugimoto, R., et al. (2008). Ex vivo carbon monoxide prevents cytochrome P450 degradation and ischemia/reperfusion injury of kidney grafts. Kidney Int. 74, 1009–1016. doi:10. 1038/ki.2008.342

National Cancer Institute (2023). Major categories of chemotherapy agents. Available online at: https://training.seer.cancer.gov/treatment/chemotherapy/types/major-categories.html (Accessed January 10, 2025).

Nguyen, K. A., Matte, A., Foresti, R., Federti, E., Kiger, L., Lefebvre, C., et al. (2024). An oral carbon monoxide–releasing molecule protects against acute hyperhemolysis in sickle cell disease. *Blood* 143, 2544–2558. doi:10.1182/blood.2023023165

Nobre, L. S., Seixas, J. D., Romão, C. C., and Saraiva, L. M. (2007). Antimicrobial action of carbon monoxide-releasing compounds. *Antimicrob. Agents Chemother.* 51, 4303–4307. doi:10.1128/AAC.00802-07

Noroozi, M., Angerson, W., and Lean, M. (1998). Effects of flavonoids and vitamin C on oxidative DNA damage to human lymphocytes. *Am. J. Clin. Nutr.* 67, 1210–1218. doi:10.1093/ajcn/67.6.1210

Noruzi, M., Zare, D., Khoshnevisan, K., and Davoodi, D. (2011). Rapid green synthesis of gold nanoparticles using Rosa hybrida petal extract at room temperature. *Spectrochim. Acta Part A Mol. Biomol. Spectrosc.* 79, 1461–1465. doi:10.1016/j.saa.2011.05.001

OECD Science (2016). Technology and innovation outlook 2016. Paris: OECD. doi:10. 1787/sti\_in\_outlook-2016-en

Omaye, S. T. (2002). Metabolic modulation of carbon monoxide toxicity. Toxicology~180,~139-150.~doi:10.1016/S0300-483X(02)00387-6

Otterbein, L. E. (2009). The evolution of carbon monoxide into medicine. Respir. Care 54, 925–932. doi:10.4187/002013209793800394

Patibandla, S., Zhang, Y., Tohari, A. M., Gu, P., Reilly, J., Chen, Y., et al. (2018). Comparative analysis of the toxicity of gold nanoparticles in zebrafish. *J. Appl. Toxicol.* 38, 1153–1161. doi:10.1002/jat.3628

Pellegrini, N., Serafini, M., Salvatore, S., Del Rio, D., Bianchi, M., and Brighenti, F. (2006). Total antioxidant capacity of spices, dried fruits, nuts, pulses, cereals and sweets consumed in Italy assessed by three different *in vitro* assays. *Mol. Nutr. Food Res.* 50, 1030–1038. doi:10.1002/mnfr.200600067

Penney, D. G., and Howley, J. W. (1991). Is there a connection between carbon monoxide exposure and hypertension? *Environ. Health Perspect.* 95, 191–198. doi:10. 1289/ehp.9195191

Peterson, R. T., Nass, R., Boyd, W. A., Freedman, J. H., Dong, K., and Narahashi, T. (2008). Use of non-mammalian alternative models for neurotoxicological study. *Neurotoxicology* 29 (3), 546–555. doi:10.1016/j.neuro.2008.04.006

Pizarro, M. D., Rodriguez, J. V., Mamprin, M. E., Fuller, B. J., Mann, B. E., Motterlini, R., et al. (2009). Protective effects of a carbon monoxide-releasing molecule (CORM-3) during hepatic cold preservation. *Cryobiology* 58, 248–255. doi:10.1016/j.cryobiol.2009. 01.002

Queiroga, C. S. F., Vercelli, A., and Vieira, H. L. A. (2015). Carbon monoxide and the CNS: challenges and achievements. *Br. J. Pharmacol.* 172, 1533–1545. doi:10.1111/bph. 12729

Ramachandran, R., Krishnaraj, C., Kumar, V. K. A., Harper, S. L., Kalaichelvan, T. P., and Yun, S.-I. (2018). *In vivo* toxicity evaluation of biologically synthesized silver nanoparticles and gold nanoparticles on adult zebrafish: a comparative study. *3 Biotech.* 8, 441. doi:10.1007/s13205-018-1457-y

Roberts, R. A., Smith, R. A., Safe, S., Szabo, C., Tjalkens, R. B., and Robertson, F. M. (2010). Toxicological and pathophysiological roles of reactive oxygen and nitrogen species. *Toxicology* 276, 85–94. doi:10.1016/j.tox.2010.07.009

Romão, C. C., Blättler, W. A., Seixas, J. D., and Bernardes, G. J. L. (2012). Developing drug molecules for therapy with carbon monoxide. *Chem. Soc. Rev.* 41, 3571. doi:10. 1039/c2cs15317c

Ryter, S. W., Alam, J., and Choi, A. M. K. (2006). Heme Oxygenase-1/Carbon monoxide: from basic science to therapeutic applications. *Physiol. Rev.* 86, 583–650. doi:10.1152/physrev.00011.2005

Ryter, S. W., Ma, K. C., and Choi, A. M. K. (2018). Carbon monoxide in lung cell physiology and disease. *Am. J. Physiol. Physiol.* 314, C211–C227. doi:10.1152/ajpcell. 00022.2017

Sadhukhan, S., Moniruzzaman, M., Maity, S., Ghosh, S., Pattanayak, A. K., Chakraborty, S. B., et al. (2022). Organometallic folate gold nanoparticles ameliorate lipopolysaccharide-induced oxidative damage and inflammation in zebrafish brain. ACS Omega 7, 9917–9928. doi:10.1021/acsomega.2c00415

Sales Junior, S. F., Vallerie, Q., de Farias Araujo, G., Soares, L. O. S., Oliveira da Silva, E., Correia, F. V., et al. (2020). Triclocarban affects earthworms during long-term exposure: behavior, cytotoxicity, oxidative stress and genotoxicity assessments. *Environ. Pollut.* 267, 115570. doi:10.1016/j.envpol.2020.115570

Sales Junior, S. F., Costa Amaral, I. C., Mannarino, C. F., Hauser-Davis, R. A., Correia, F. V., and Saggioro, E. M. (2021). Long-term landfill leachate exposure modulates antioxidant responses and causes cyto-genotoxic effects in *Eisenia andrei* earthworms. *Environ. Pollut.* 287, 117351. doi:10.1016/j.envpol.2021.117351

Sales Junior, S. F., da Costa, N. M., de Farias Araújo, G., Soares, L. O. S., Mannarino, C. F., Correia, F. V., et al. (2024). Antioxidant system alterations, oxidative, and genotoxic effects in *Danio rerio* (zebrafish) exposed to leachate from a dumpsite. *Environ. Sci. Pollut. Res.* 31, 10737–10749. doi:10.1007/s11356-024-31883-4

Sangwan, S., and Seth, R. (2022). Synthesis, characterization and stability of gold nanoparticles (AuNPs) in different buffer systems. *J. Clust. Sci.* 33, 749–764. doi:10. 1007/s10876-020-01956-8

Sawicka, M., Drągowski, P., Stelmaszewska, J., Prokop, I., Sawicki, K., Polityńska, B., et al. (2022). Cell viability and collagen metabolism of MCF-7 breast cancer cells are affected by carbon monoxide released from CORM-2. *Acta Pol. Pharm. - Drug Res.* 79, 475–486. doi:10.32383/appdr/153012

Schaeublin, N. M., Braydich-Stolle, L. K., Schrand, A. M., Miller, J. M., Hutchison, J., Schlager, J. J., et al. (2011). Surface charge of gold nanoparticles mediates mechanism of toxicity. *Nanoscale* 3, 410. doi:10.1039/c0nr00478b

Schatzschneider, U. (2015). Novel lead structures and activation mechanisms for CO -releasing molecules (CORMs). *Br. J. Pharmacol.* 172, 1638–1650. doi:10.1111/bph.

Shankar, S. S., Rai, A., Ankamwar, B., Singh, A., Ahmad, A., and Sastry, M. (2004). Biological synthesis of triangular gold nanoprisms. *Nat. Mater.* 3, 482–488. doi:10.1038/nmat1152

Sharma, S., Parveen, R., and Chatterji, B. P. (2021). Toxicology of nanoparticles in drug delivery. *Curr. Pathobiol. Rep.* 9 (9), 133–144. doi:10.1007/s40139-021-00227-z

Shukla, R. K., Badiye, A., Vajpayee, K., and Kapoor, N. (2021). Genotoxic potential of nanoparticles: structural and functional modifications in DNA. *Front. Genet.* 12, 728250. doi:10.3389/fgene.2021.728250

Simon, T., Potara, M., Gabudean, A.-M., Licarete, E., Banciu, M., and Astilean, S. (2015). Designing Theranostic agents based on pluronic stabilized gold nanoaggregates loaded with methylene blue for multimodal cell imaging and enhanced photodynamic therapy. ACS Appl. Mater. Interfaces 7, 16191–16201. doi:10.1021/acsami.5b04734

Sokolsky-Papkov, M., and Kabanov, A. (2019). Synthesis of well-defined gold nanoparticles using pluronic: the role of radicals and surfactants in nanoparticles formation. *Polym. (Basel)* 11, 1553. doi:10.3390/polym11101553

Southam, H. M., Williamson, M. P., Chapman, J. A., Lyon, R. L., Trevitt, C. R., Henderson, P. J. F., et al. (2021). Carbon-monoxide-releasing Molecule-2 (CORM-2)' is a misnomer: ruthenium toxicity, not CO release, accounts for its antimicrobial effects. *Antioxidants* 10, 915. doi:10.3390/antiox10060915

Souza, J. P., Mansano, A. S., Venturini, F. P., Marangoni, V. S., Lins, P. M. P., Silva, B. P. C., et al. (2021). Toxicity of gold nanorods on Ceriodaphnia dubia and *Danio rerio* after sub-lethal exposure and recovery. *Environ. Sci. Pollut. Res.* 28, 25316–25326. doi:10.1007/s11356-021-12423-w

- Strigul, N., Vaccari, L., Galdun, C., Wazne, M., Liu, X., Christodoulatos, C., et al. (2009). Acute toxicity of boron, titanium dioxide, and aluminum nanoparticles to Daphnia magna and Vibrio fischeri. *Desalination* 248, 771–782. doi:10.1016/j.desal. 2009.01.013
- Tahir, Concas, G. C., Gisbert, M., Cremona, M., Lazaro, F., Maia da Costa, M. E. H., et al. (2024). Pulsed-laser-driven CO 2 reduction reaction for the control of the photoluminescence quantum yield of organometallic gold nanocomposites. *Small Sci.* 4, 2300328. doi:10.1002/smsc.202300328
- Tian, H., Chen, H., Yin, X., Lv, M., Wei, L., Zhang, Y., et al. (2024). CORM-3 inhibits the inflammatory response of human periodontal ligament fibroblasts stimulated by LPS and high glucose. *J. Inflamm. Res.* 17, 4845–4863. doi:10.2147/IIR.S460954
- Torres, C. A., Mendes, N. V., Baldin, S. L., Bernardo, H. T., Vieira, K. M., Scussel, R., et al. (2021). Cotreatment of small gold nanoparticles protects against the increase in cerebral acetylcholinesterase activity and oxidative stress induced by acute ethanol exposure in the zebrafish. *Neuroscience* 457, 41–50. doi:10.1016/j.neuroscience.2021. 01.011
- Tournebize, J., Boudier, A., Joubert, O., Eidi, H., Bartosz, G., Maincent, P., et al. (2012). Impact of gold nanoparticle coating on redox homeostasis. *Int. J. Pharm.* 438, 107–116. doi:10.1016/j.ijpharm.2012.07.026
- Truong, L., Tilton, S. C., Zaikova, T., Richman, E., Waters, K. M., Hutchison, J. E., et al. (2013). Surface functionalities of gold nanoparticles impact embryonic gene expression responses. *Nanotoxicology* 7, 192–201. doi:10.3109/17435390.2011.648225
- Tsai, S.-W., Liaw, J.-W., Kao, Y.-C., Huang, M.-Y., Lee, C.-Y., Rau, L.-R., et al. (2013). Internalized gold nanoparticles do not affect the osteogenesis and apoptosis of MG63 osteoblast-like cells: a quantitative, *in vitro* study. *PLoS One* 8, e76545. doi:10.1371/journal.pone.0076545
- Tsikas, D. (2017). Assessment of lipid peroxidation by measuring malondialdehyde (MDA) and relatives in biological samples: analytical and biological challenges. *Anal. Biochem.* 524, 13–30. doi:10.1016/j.ab.2016.10.021
- Verma, S. K., Jha, E., Panda, P. K., Kumari, P., Pramanik, N., Kumari, S., et al. (2018). Molecular investigation to RNA and protein based interaction induced *in vivo* biocompatibility of phytofabricated AuNP with embryonic zebrafish. *Artif. Cells, Nanomedicine, Biotechnol.* 46, 671–684. doi:10.1080/21691401.2018.1505746
- Volti, G. L., Sacerdoti, D., Sangras, B., Vanella, A., Mezentsev, A., Scapagnini, G., et al. (2005). Carbon monoxide signaling in promoting angiogenesis in human microvessel endothelial cells. *Antioxid. Redox Signal.* 7, 704–710. doi:10.1089/ars.2005.7.704

- Vona, R., Gambardella, L., Cittadini, C., Straface, E., and Pietraforte, D. (2019). Biomarkers of oxidative stress in metabolic syndrome and associated diseases. *Oxid. Med. Cell. Longev.* 2019, 1–19. doi:10.1155/2019/8267234
- Wendy Underwood, R. A. (2020). AVMA guidelines for the euthanasia of animals: 2020 edition. 2020th Edn. Illinois: American Veterinary Medical Association.
- Wilhelm Filho, D., Torres, M. A., Zaniboni-Filho, E., and Pedrosa, R. C. (2005). Effect of different oxygen tensions on weight gain, feed conversion, and antioxidant status in piapara, leporinus elongatus (valenciennes, 1847). *Aquaculture* 244, 349–357. doi:10. 1016/j.aquaculture.2004.11.024
- Wu, G., Lupton, J. R., Turner, N. D., Fang, Y.-Z., and Yang, S. (2004). Glutathione metabolism and its implications for health. *J. Nutr.* 134, 489–492. doi:10.1093/jn/134.3.489
- Xu, Z., Kusumbe, A. P., Cai, H., Wan, Q., and Chen, J. (2023). Type H blood vessels in coupling angiogenesis-osteogenesis and its application in bone tissue engineering. *J. Biomed. Mater. Res. Part B Appl. Biomater.* 111, 1434–1446. doi:10. 1002/jbm.b.35243
- Xue, Y., Li, X., Li, H., and Zhang, W. (2014). Quantifying thiol-gold interactions towards the efficient strength control. *Nat. Commun.* 5, 4348. doi:10.1038/ncomms5348
- Yan, S., Wang, J., Zhu, L., Chen, A., and Wang, J. (2015). Toxic effects of nitenpyram on antioxidant enzyme system and DNA in zebrafish (*Danio rerio*) livers. *Ecotoxicol. Environ. Saf.* 122, 54–60. doi:10.1016/j.ecoenv.2015.06.030
- Yan, S. H., Wang, J. H., Zhu, L. S., Chen, A. M., and Wang, J. (2016). Thiamethoxam induces oxidative stress and antioxidant response in zebrafish (*Danio Rerio*) livers. *Environ. Toxicol.* 31, 2006–2015. doi:10.1002/tox.22201
- Yoshida, J., Ozaki, K. S., Nalesnik, M. A., Ueki, S., Castillo-Rama, M., Faleo, G., et al. (2010). *Ex vivo* application of carbon monoxide in UW solution prevents transplant-induced renal ischemia/reperfusion injury in pigs. *Am. J. Transpl.* 10, 763–772. doi:10. 1111/j.1600-6143.2010.03040.x
- Yuan, Z., De La Cruz, L. K., Yang, X., and Wang, B. (2022). Carbon monoxide signaling: examining its engagement with various molecular targets in the context of binding affinity, concentration, and biologic response. *Pharmacol. Rev.* 74, 825–875. doi:10.1124/pharmrev.121.000564
- Zhang, W.-Q., Atkin, A. J., Thatcher, R. J., Whitwood, A. C., Fairlamb, I. J. S., and Lynam, J. M. (2009). Diversity and design of metal-based carbon monoxide-releasing molecules (CO-RMs) in aqueous systems: revealing the essential trends. *Dalt. Trans.* 4351, 4351–4358. doi:10.1039/b822157j
- Zheng, M., Liu, Y., Zhang, G., Yang, Z., Xu, W., and Chen, Q. (2023). The applications and mechanisms of superoxide dismutase in medicine, food, and cosmetics. *Antioxidants* 12, 1675. doi:10.3390/antiox12091675